

UNCLASSIFIED

AD

401 482

*Reproduced
by the*

DEFENSE DOCUMENTATION CENTER

FOR

SCIENTIFIC AND TECHNICAL INFORMATION

CAMERON STATION, ALEXANDRIA, VIRGINIA



UNCLASSIFIED

NOTICE: When government or other drawings, specifications or other data are used for any purpose other than in connection with a definitely related government procurement operation, the U. S. Government thereby incurs no responsibility, nor any obligation whatsoever; and the fact that the Government may have formulated, furnished, or in any way supplied the said drawings, specifications, or other data is not to be regarded by implication or otherwise as in any manner licensing the holder or any other person or corporation, or conveying any rights or permission to manufacture, use or sell any patented invention that may in any way be related thereto.

401 482

IN ORDER TO FURNISH INFORMATION

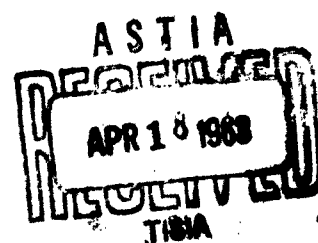
CATALOGED BY ASTIA
AS AD NO. 401482

63-32
Welded Continuous Frames and Their Components



EXPERIMENTS ON BRACED WIDE-FLANGED BEAMS

by
G. C. Lee
A. T. Ferrara
T. V. Galanboe



Fritz Engineering Laboratory Report No. 205 H.6

Welded Continuous Frames and Their Components

EXPERIMENTS ON BRACED WIDE-FLANGE BEAMS

by

G. C. Lee, A. T. Ferrara and T. V. Galambos

This work has been carried out as part of an investigation sponsored jointly by the Welding Research Council and the Department of the Navy with funds furnished by the following:

American Institute of Steel Construction
American Iron and Steel Institute
Office of Naval Research (Contract No. 61003)
Bureau of Ships
Bureau of Yards and Docks

Reproduction of this report in whole or in part is permitted for any purpose of the United States Government.

Fritz Engineering Laboratory
Lehigh University
Bethlehem, Pennsylvania

March 1963

Fritz Engineering Laboratory Report No. 205H.6.

SYNOPSIS

This report contains a description of fourteen experiments on wide-flange beams braced by purlins. These experiments were performed to study the bracing requirements of plastically designed beams. All fourteen beams performed in a satisfactory manner by delivering a plastic hinge of sufficient rotation capacity. The results indicate that beam bracing members need to possess only nominal bending stiffness. Failure in each test was precipitated by combined local and lateral-torsional buckling.

TABLE OF CONTENTS

	Page No.
SYNOPSIS	i
TABLE OF CONTENTS	ii
1. INTRODUCTION	1
2. DESCRIPTION OF THE EXPERIMENTAL PROGRAM	5
2.1 Objectives	5
2.2 Spacing of the Bracing	6
2.3 Test Program	8
2.4 Test Set-Up	10
2.5 Instrumentation	12
2.6 Material Properties	14
3. DISCUSSION OF THE EXPERIMENTAL RESULTS	15
3.1 Load-Deformation Behavior	15
3.2 The Failure of Braced Beams	20
3.3 The Role of the Purlins	22
3.4 The Influence of Instability	26
4. SUMMARY AND CONCLUSIONS	30
4.1 Plastic Hinge Behavior	30

4.2	Influence of the Variation of the Test Parameters	32
4.3	Additional Recommended Research	33
4.4	Influence of Test Results on Design	36
5.	ACKNOWLEDGEMENTS	38
6.	NOMENCLATURE	39
7.	TABLES AND FIGURES	40
8.	REFERENCES	

1. INTRODUCTION

The proper proportioning of lateral bracing is of great importance in the design of steel structures, particularly when the design is based on the principles of plastic theory. In plastic design a given member must not only be capable of supplying its full plastic moment M_p , but it usually must also sustain this moment through a certain amount of inelastic rotation.

Ample experimental evidence exists which indicates that beam elements in continuous structures can behave as assumed in simple plastic theory⁽¹⁾. This means that the first hinge to form in the structure is capable of rotating without a drop in the plastic moment until the last hinge has developed and the structure fails as a mechanism. This ideal performance is achieved, however, only if the detrimental effects of instability can be prevented from influencing the inelastic rotation capacity of the member.

Desirable and undesirable rotation behavior is illustrated in Fig. 1, where a simply supported beam is subjected to two symmetrically placed concentrated loads such that the

central portion of the beam is under uniform moment. The two curves in Fig. 1 show the relationship between the moment in the central segment of the wide-flange beam and the slope at the end of this segment ($M - \theta$ curves). In plastic design it is necessary that the $M - \theta$ curve possesses a flat plateau at the level of M_p (solid curve in Fig. 1) before failure occurs by a reduction of the moment capacity. In a properly braced beam this reduction is usually triggered by local buckling. The flat portion of the $M - \theta$ curve must be of sufficient length to permit hinge formation elsewhere in the structure of which the beam element shown in Fig. 1 is a part. Undesirable performance is usually the result of improper bracing, and it is characterized by the absence of a hinge plateau, as shown by the dashed curve in Fig. 1. In this case no plastic hinge exists, and the $M - \theta$ curve unloads as soon as lateral buckling occurs.

There are two instability phenomena that occur in steel wide-flange members which are subjected to forces causing bending about the major axis of the section: lateral buckling and local buckling. These buckling phenomena are inherent weaknesses of the wide-flange shape, and they cannot ultimately be prevented from occurring. Despite these congenital deficiencies,

however, wide-flange beams can be made to behave in a satisfactory manner.

It has been observed⁽²⁾ during experiments on beams loaded as shown in Fig. 1 that lateral buckling started as soon as the full plastic moment was reached, regardless of the spacing of the bracing. This did not, however, precipitate failure. The members continued to deform without a drop in moment capacity, provided the lateral bracing was spaced at less than or equal to a certain critical distance. Failure finally occurred in these beams after local buckling of the flanges had set in and at rotations sufficiently large to justify use of the members in plastically designed structures.

The following problems can now be formulated:

- 1) What must be the spacing of the lateral bracing in order to attain satisfactory behavior?
- 2) What is the required stiffness of this bracing?
- 3) What are the maximum width-thickness ratios required to force local buckling to occur at strains large enough to permit the full development of a plastic hinge.

The last of these problems, that is the local buckling problem, has been considered⁽³⁾, and it was found that the width-thickness ratios of the plate elements in most rolled wide-flange shapes were satisfactory, and that sufficient inelastic rotation can be expected in bending if the width thickness ratios did not exceed the following values: $b/t = 17$ and $d/w = 70$.

The problem of the spacing of lateral bracing in plastically designed structures has been investigated theoretically and experimentally⁽²⁾⁽³⁾⁽⁴⁾⁽⁵⁾, and specifications based on this research are now in use⁽⁶⁾. However, no information was available on the minimum requirements of the stiffness of this bracing. The problem has been studied for elastic structures⁽⁷⁾⁽⁸⁾, but it was found necessary to perform some experiments for the inelastic range. These experiments were conducted in 1961 and 1962 at Lehigh University. This report contains a description of the tests and a discussion of the experimental results.

2. DESCRIPTION OF THE EXPERIMENTAL PROGRAM

2.1 OBJECTIVES

A series of fourteen experiments were performed in this program to study the behavior of braced beams. The structure used in these tests was a simply supported wide-flange beam which was loaded by two symmetrically spaced lateral loads such that the central portion of the beam was subjected to uniform moment. Bending was about the major axis of the rolled steel beam. A schematic view of the test structure is shown in the inset of Fig. 1; the actual structure is shown in Fig. 2. It was found convenient to apply the loads at the ends and to provide the reaction support in the interior of the span, thus turning the structure so that the compression flange was at the bottom. The resulting moment diagram is the same in either case, and it is shown in the lower part of Fig. 2.

Lateral bracing was provided at the ends of the member and under the load points, thus subdividing the beam into three unbraced fields. The two outside spans remained essentially elastic and were each of length L_{adj} . These spans are termed the "adjacent spans". The central portion is the critical span

because it is subjected to uniform moment. This span was fully yielded under the plastic moment M_p .

Lateral bracing at the ends consisted of two knife-edge guides which permitted free transverse deflection and rotation, free lateral rotation and free warping, but they prevented twisting and lateral deflection. The lateral bracing at the load points bracketed the critical segment of the beam, and it consisted of purlin members which framed into the compression flange of the beam at right angles.

The principal objective of the experiments was to determine the minimum dimensions of the purlin members required to still permit the braced beam to deliver a plastic hinge. Other objectives were: (1) to observe the post-yielding behavior of beam-purlin assemblies in order to furnish data for later theoretical work, (2) to study the effectiveness of various methods of attaching the purlins to the beam, (3) to study the effect of varying the length of the adjacent span, and (4) to investigate the effectiveness of the vertical stiffeners at the points of lateral support.

2.2 SPACING OF THE BRACING

The problem of the proper spacing of the bracing was

considered in a previous test program⁽²⁾. In this study the experiments were performed on the same structure as in the present investigation (Fig. 2.) with the exception that the purlins under the load point were replaced by knife-edge guides which permitted lateral rotation but prevented lateral deflection and twisting.

The only experimental variable was the length of the critical span. Four tests were performed, with $L_{cr} = 35r_y$, $40r_y$, $45r_y$ and $50r_y$ (where r_y is the least radius of gyration). In each case the adjacent span length was kept equal to the length of the critical span. The results of the tests were as follows: all but the longest beam ($L_{cr} = 50r_y$) delivered a plastic hinge of at least ten times the rotation at the initiation of yielding.

These tests showed that for the type of structure and loading which was investigated one could expect a plastic hinge to form if the critical span was no longer than $45r_y$. Since a uniform moment on the critical span is the most severe condition which one could encounter in plastic design, it was decided to test the same type of structure for the present study on the

required bracing. The critical length for all of these tests was taken as $40r_y$.

2.3 TEST PROGRAM

The details of the test program are listed in Table 1. A total of 14 experiments were performed, and the breakdown of the variables is as follows:

Main beams: With the exception of P-3 and P-4 these were all 10WF25 shapes. The former were 8B13 shapes, and the different section for these was chosen to find out if significantly different behavior resulted from selecting a section which is more critical with regard to local buckling. The length of the critical span was in each case $40r_y$. In all except P-6 the length of the adjacent span was equal to the length of the critical span. The adjacent span for P-6 was $60r_y$.

Purlin Members: In tests LB-12, LB-13, and LB-14 the size of purlins was varied while their length was kept constant. In tests LB-18, LB-19, and LB-20 the length of the purlins was varied while their size was kept constant. The purlins for most of the other tests were chosen to give a length-to-depth ratio of 28.

The purlin lengths for LB-22 and P-10 were somewhat shorter ($l/d = 18.7$) because purlins were provided on one side only. This bracing condition simulates an end-frame in a multi-frame structure. All other purlins extended an equal length on both sides of the beam. The purlins were all pinned at their far end to fixtures which were tied to the laboratory floor.

Beam-to-purlin connections: Purlins for all tests except LB-22, P-6, P-8 and P-10 were one piece, going through under the main beam. In test P-7 the purlins were bolted to the beam by four 3/8-in. bolts. In all the other tests the purlins were fillet welded to the outside face of the compression flange of the main beam. In tests P-6 and P-8 the purlins were discontinuous (that is, two separate purlins), in P-6 they were welded on and in P-8 they were bolted on. In tests LB-22 and P-10, where purlins were provided on one side only, the purlins were welded on for LB-22 and bolted on for P-10. In all continuous purlins stiffeners were added in the plane of the web of the main member. Details of the various beam-to-purlin connections are shown in Fig. 3.

Vertical Stiffeners: Full vertical stiffeners were

welded to the main beam at all points of lateral support. Details of these stiffeners can be seen in Fig. 3. These stiffeners were present in all the specimens except in test P-9, where the stiffeners at the purlin points extended only halfway, thus stiffening only the compression flange and half of the web. This experiment was performed to determine whether full stiffeners might be omitted in plastically designed beams. This stiffener detail can be clearly seen in Fig. 6.

2.4 TEST SET-UP

Various views of the test set-up are shown in Figs. 4a, b, c, and d. The two vertical support rods at the purlin points, as well as the two hydraulic jacks which supplied the loads to the ends of the beam, reacted against a stiff overhead supporting girder. This girder was supported by the cross-beams of two rectangular frames. The supporting columns for these frames were bolted to the laboratory floor (Fig. 4c).

The loads were applied at the ends of the test beam by means of two hydraulic jacks. These jacks were on a parallel pressure circuit and therefore they supplied equal downward forces. The hydraulic pressure was furnished by an Amsler pendulum dynamometer which also measured the magnitude of the

applied loads. To simulate knife-edge loading, the loads were transmitted from the jacks to the beams through 2-in. diameter rollers (Fig. 4a and c).

The vertical supports at the purlin points (at the ends of the critical span) were 1-in. diameter high-strength steel rods. These rods were connected by an articulated joint to the overhead supporting girder at their top. At the bottom the vertical rod was pin-connected to the test beam either through two plates welded to the tension flange (tests LB-12, LB-13, LB-14, LB-22, P-6, P-8 and P-10) or through a yoke which transmitted the forces to the compression flange (all other tests). In the latter case the load was carried through the yoke by means of four high-strength steel rods to a 1-in. thick plate on the compression side of the beam. The load was further transmitted to the test beam by means of a roller placed parallel to the longitudinal axis of the beam between the plate and the beam in such a manner that the vertical support did not restrain the cross section from twisting. Further details of these two loading arrangements are visible in the photographs of Figs. 5 and 6.

Lateral Supports: The lateral supports at the ends of the test beam consisted of two 1/2-in. plates which were bolted to the webs of two 5-in. deep channels. These channels were in turn welded to a base plate which was bolted to a heavy base beam. This beam was anchored to the laboratory floor. To create a knife-edge condition, 1/2-in. diameter rods were welded to the edges of the plates, and before each test, grease was applied along the contact points of this rod with the flanges of the test beam to keep friction to a minimum. Details of these lateral supports can be seen in Figs. 4b and c.

Lateral support at the ends of the critical span was provided by purlin members framing into the outside face of the compression flange at right angles. Details of the beam-to-purlin connections have been described earlier. The drawings in Figs. 4b and 4d show the layout of this bracing system, and an overall view is given in Fig. 7, where the photograph shows test P-8 in progress.

2.5 INSTRUMENTATION

Deflections and curvatures in the loading and lateral direction were measured during each test. In the elastic range readings were taken for convenient increments of load, while in

the inelastic range increments of deformation were used. Loading was stopped each time readings were taken.

In the inelastic range the readings were not taken until sufficient time had elapsed to permit the system to come to rest, and therefore the effects of rate of loading do not influence the results and the test points in the curves in Figs. 9 to 10 represent stable deflection configurations for static loading.

Vertical deflections of the test specimen were measured by means of a surveyor's level and a travelling 1/100-in. scale that was held vertically at each of thirteen points laid out across the entire length of the beam. Lateral deflections were measured by means of a transit fixed in a vertical plane and a 1/100-in. travelling scale. Lateral deflections of both the compression and tension flange were recorded.

Curvature of the test beam was obtained from strain readings in the plane of the web and from section geometry. Strains were obtained from pairs of SR-4 gages placed as shown in Fig. 8. The gages at the flange tips were used to determine the start of lateral buckling since this caused a significant

difference in strain on the opposite tips of the compression flange. At each end of the critical span, slope-measuring devices were used. These devices can be seen in Fig. 5. A 15-in. steel rod was connected to the stiffener and thus rotated with the test beam. The amount of rotation was measured by two Ames Dials connected to the ends of the rod by thin steel wire. The dial readings furnished the slopes at each end of the critical span, and since there was theoretically a constant moment across the span, the curvature was obtained by dividing the change in slope by the length. The values of curvature so obtained were used as a check on those calculated using the strain readings, and the two compared favorably.

2.6 MATERIAL PROPERTIES

The test specimens were rolled 10WF25 and 8B13 sections of ASTM A7 structural steel. They were produced in three separate rollings: two for the 10WF25 and one for the 8B13 section. Three series of tensile coupon tests were made for each of the three heats to determine the material properties. Coupons were cut from the webs and the flanges of the cross sections. The yield stress in the flanges (σ_{yf}) and in the web (σ_{yw}) are listed in Table 2 for each specimen. The plastic moment of the sections

was computed by the formula:

$$M_{p1} = bt (d-t) \sigma_{yf} + \frac{w}{4} (d-2t)^2 \sigma_{yw} \quad (1)$$

to account for the differences in yield stress between the web and the flanges. Average measured dimension b , t , d , and w were used for each specimen, and the calculated plastic moments are listed in Table 2. These values (M_{p1}) were used in non-dimensionalizing the results of the experiments.

In addition to the coupon tests, three short beam tests were performed to determine the plastic moment experimentally. The length of the short beams was $20r_y$ and the measured plastic moments are given as M_{p2} in Table 2.

Nominal section properties of all beam and purlin sections used in this program are tabulated in Table 3.

3. DISCUSSION OF THE EXPERIMENTAL RESULTS

3.1 LOAD-DEFORMATION BEHAVIOR

There are three types of deformations which can be considered in the comparative study of the behavior of the test specimens: (1) the deformations in the vertical plane (which was also the plane in which the loads were applied), (2) the

lateral deflections or the twisting of the member, and (3) the local buckling deformations. By comparing the load-deformation curves, one can draw conclusions about the influence of the variation of the test parameters.

The curvature at the midspan of the critical segment will be used in the following parts of this report as an index of the behavior in the vertical plane. The vertical deflections at midspan or the slope at the ends of the critical span could just as well have been used.

The curvature was computed as the average curvature obtained from the strains recorded by three pairs of strain gages located at and two inches away from the mid section of each beam (sections AA, BB and CC in Fig. 8). These strain gages were located in the plane of the web on the outside faces of the flanges. The resulting curvature is, strictly speaking, not the curvature in the vertical plane, but the curvature in the plane of the web. The curvature in the vertical plane is equal to the curvature in the plane of the web times the cosine of the angle of twist. The cosine of the largest recorded angle of twist was, however, greater than 0.98, and therefore

the two curvatures can be considered identical for all practical purposes.

The test results for the load-deformation behavior in the vertical plane are presented in Figs. 9 to 15. In Fig. 9 the moment-versus compression and tension flange strains are shown for test LB-18. A complete moment-curvature curve for test LB-18 is given in Fig. 10. The curves in Figs. 11 to 15 show the inelastic portion of the $M-\phi$ curve for each test. Included among these is also the curve for test LB-15 from the previous test program⁽²⁾. This test was in all respects identical to the tests in this test series ($L_{cr} = L_{adj} = 40r_y$; A-7 steel, 10WF25 section), except that the bracing at the ends of the critical span was not furnished by purlins but by knife-edge guides.

The $M-\phi$ curves in Figs. 10 to 15 are non-dimensionalized as follows: The moment (the ordinate) is divided by the plastic moment, M_p , which was computed by Eq. 1. The curvature (the abscissa) is divided by the curvature at the theoretical initiation of yielding, $\phi_y = \frac{2\sigma_{yf}}{E}$.

The load-deformation behavior in the lateral direction

is illustrated in Figs. 16 to 19 by moment-versus-twisting angle curves. In Fig. 16 a typical set of curves is shown for test LB-18. The curve on the left is for the lateral deflection of the compression flange, u_c ; the curve in the center gives the lateral deflection of the tension flange u_t ; and the right curve shows the variation of the angle of twist, β . The relationship between u_c , u_t and β is shown by the sketch in this figure. The curves in Figs. 17 to 19 show the twist β of the section at the center of the critical segment.

The complete curves are shown in Fig. 16 as an example, and the inelastic portions of the $M=\beta$ curves are given in Fig. 17 to 19 for each test, including LB-15.

Since it was not known a priori where local buckling would occur, no measurements were made on the change in the shape of the cross section. Local buckling was observed visually, and the load-point at which local buckling first was observed is noted on each curve in Figs. 10 to 19 by an arrow and by the symbol B. At these locations local buckling, which occurred in each test in the compression flange, was definitely present. Since it was possible to clearly note the start of

local buckling by visual observation of the flange tips, it is also certain that local buckling was not present at the load-point before. Thus local buckling commenced between the load-point marked B and the point directly before it.

Also shown in each curve in Figs. 10 to 16 is the start of lateral buckling. This point is located by an arrow and the symbol A. The start of lateral buckling was noted from a distinct lateral movement of the compression flange (see $M-u_c$ curve in Fig. 16), and from the change in the strain readings in the SR-4 gages located at the tips of the flanges at midspan (Fig. 8).

Because of the fact that local buckling could be considered the point of failure in many of the experiments, the deflected shape of the compression flange at the start of local buckling (B in Figs. 10 to 19) is also of interest. The deflected shape of the compression flange along the whole length of the beam is given for each test in Figs. 20 to 22.

The experimental data have now been presented: $M-\phi$ curves in Figs. 10 to 15, $M-\beta$ curves in Figs. 16 to 19, and the deflected shapes at the start of local buckling in Figs.

20 to 23. Following is a discussion of the significance of these test results.

3.2 THE FAILURE OF BRACED BEAMS

All tested beam-purlin assemblies behaved in a very similar manner during the complete loading history. Upon the application of the first few loads the beams responded elastically. The $M-\phi$ relationship was linear (see Fig. 10), and no lateral deflections were observed. Above approximately $0.8 M_p$, yielding commenced due to the presence of residual stresses, and the $M-\phi$ curves became non-linear. Each $M-\phi$ curve exhibited such a "knee" which finally flattened out when the whole cross section became plastified.

Each test specimen furnished a "hinge plateau" at or near the value of M_p computed from the previously measured material and cross sectional properties, as can be seen from the $M-\phi$ curves of Figs. 11 to 15. There are some variations in the level of the experimental plastic moment; however, these are not large (the maximum is $1.07 M_p$ for LB-20 and the minimum is $0.93 M_p$ for P-3), and they can be attributed to minor variations in material and sectional properties. Thus each test did deliver a plastic hinge of some length.

Soon after full plastification of the critical segment, lateral buckling was observed in all the tests. This phenomenon occurred near a curvature of $3 \phi_y$, with a variation ranging from $1.5 \phi_y$ for P-6 and $5.3 \phi_y$ for LB-20. Despite the presence of lateral buckling, no unloading of the moment was observed. As the deformation was increased, the beams continued to hold the moment while deforming both in the vertical plane and in the lateral direction. This can be seen from the sketch of the compression flange of the critical segment of the beam in Fig. 23. The top sketch in this figure shows the distribution of the yield lines at the outside face of the compression flange at the start of lateral buckling. The yield lines were relatively evenly spaced. As vertical deflection was increased, all of the shortening of the compression flange was due to lateral movement. No new yield lines which spanned across the whole width of the flange appeared. However, new yield lines appeared in that region of the compression flange which was further compressed by the lateral buckling process. The distribution of the yield lines just prior to local buckling is illustrated by the lower sketch in Fig. 23. Local buckling occurred always in the newly yielded region, and it started at the flange tip. Its inception could be readily observed by the appearance of

small waves in the flange. After lateral buckling the purlins also began to deform in the horizontal plane.

The start of local buckling could be considered the start of failure for many of the experiments (LB-18, LB-22, P-6, P-7, P-8, for example). However, for some, the beam continued to support the moment (P-4 and P-9, for example) despite the presence of both local and lateral buckling, and even for those tests where local buckling initiated unloading, this process was gradual and it could by no means be considered catastrophic. In some of the tests (LB-15 and LB-19 for example) one could argue that unloading began before local buckling. However, in these tests the point of failure is just one load point before the recorded onset of buckling. It was pointed out earlier that local buckling could occur between these two points, and thus unloading for these two tests is also due to local buckling.

3.3 THE ROLE OF THE PURLINS

The purlins which were attached to the compression flange of each test beam at the ends of the critical span acted as effective lateral braces, because each beam was able to sustain the full plastic moment through a certain amount of inelastic

rotation. The action of the purlins was two-fold: (1) they prevented the lateral movement of the compression flange at the bracing points, and (2) they helped, along with the elastic compression flange of the adjacent beam span, to restrain the lateral rotation of the compression flange at the ends of the critical span.

The first action, that is keeping the point of bracing fixed in the lateral direction, was performed very well by most of the purlins, as can be seen by observing the lateral deflected shapes of the compression flanges in Figs. 20 to 22. These curves represent the shape of the flange centerline at the point of observed local buckling. For most of the tests the purlin points moved hardly at all, or very little (on the order of 0.1 in.) except for tests LB-22 and P-10 where purlins were present on one side only. In these two tests, especially on the left purlin of LB-22, the movement of the purlin point was considerable. Despite this fact, however, a plastic hinge was delivered.

The second action, that of providing an elastic restraint to the lateral deformation of the critical compression flange, was quite small, and it is not a necessary function of the purlins. It was shown in the previous test-program⁽²⁾

that the adjacent span is quite sufficient for providing the necessary stiffness. In these tests (one of these was LB-15, the deflected shape of which is shown in Fig. 20) the purlins were replaced by knife-edges, which provided no restraint against the lateral rotation of the compression flange.

An estimate of the relative magnitude of the lateral restraint at the ends of the critical span can be made by assuming that this restraint is furnished by the purlins, which remained elastic in all of the tests (as evidenced by the absence of yield lines on the coat of whitewash and from strain gage readings in one test), and by the compression flange of the adjacent spans. The deformed shape of the top of the beam-purlin assembly is shown in Fig. 24. The stiffness of the adjacent spans is equal to

$$\frac{M}{\theta} = \frac{3EI_y B}{2L_B}$$

and the stiffness of one purlin is equal to

$$\frac{M}{\theta} = \frac{3EI_y P}{L_P}$$

The relative stiffness is defined as

$$S_{ADJ} = \frac{M}{3E\theta} = \frac{I_y B}{2L_B} \quad (2)$$

$$S_{PURLINS} = \frac{M}{3E\theta} = \frac{2I_y P}{L_P} \quad (3)$$

In Eq. 2, S_{ADJ} is the relative stiffness of the compression flange of the adjacent span, and in Eq. 3, $S_{PURLINS}$ is the same quantity for the two purlins. The total relative stiffness is equal to:

$$S = S_{ADJ} + S_{PURLINS} \quad (4)$$

The computed values of S_{ADJ} , $S_{PURLINS}$ and S are tabulated in Table 4 for all of the experiments. It can be seen from this list that the contribution of the purlins is small when compared to the contribution of the adjacent span. One could conclude from this that even the seemingly large variations in purlin stiffness of these tests would have a small influence of the behavior of the critical span, as long as the purlins are able to keep the point of support from moving laterally.

This is indeed so, as can be seen from Fig. 25, in which the total stiffness S , is plotted against the vertical plane curvature at the start of local buckling (upper portion of Fig. 25) and against the lateral deflection of the compression flange, $\frac{u_c}{L}$, at the start of local buckling (lower portion of Fig. 25). These values of ϕ/ϕ_y , $\frac{u_c}{L}$, as well as the midspan twist β/L are also tabulated in Table 4. The scatter of the points in Fig. 25 indicates that there is no distinguish-

able regular trend between the failure behavior of the beam and the lateral stiffness of the purlins.

3.4 THE INFLUENCE OF INSTABILITY

Two types of inelastic instability were observed in these experiments: lateral buckling and local buckling. Despite the presence of bracing and despite the fulfillment of the required width-thickness provisions, the two types of instability occurred. It was also obvious from these tests that the two phenomena were interrelated. Lateral buckling had occurred first in each case, and local buckling followed in locations of increased compression caused by lateral buckling. Thus the mechanism of failure by local buckling is not the same as failure obtained by uniformly compressing the compression flange. It is rather the case of the failure of a bent beam which is also subjected to an axial stress.

Lateral buckling was not observed to be directly responsible for failure. Before local buckling the beams did not show any signs of unloading.* Also, the onset of lateral buck-

* For unbraced lengths larger than $45r_y$, this is not true any more, because it was observed in Ref. 2 that unloading was caused by lateral buckling for a beam with $L/r = 50$.

ling is quite easily predicted. It occurs when the full cross section is yielded, at curvatures of approximately 2 to 4 ϕ_y .

Unfortunately the prediction of the occurrence of local buckling is not obvious from the test results obtained here. Since one could assume that the onset of local buckling was the cause of failure in most of the test beams, it is important that this should be known.

An examination of the scattered points in Fig. 25 reveals that there is, within the range of end stiffnesses considered here, no detectable influence of the variation of the stiffnesses on the onset of local buckling. To check interdependence of local and lateral buckling, the amount of midspan lateral deflection is plotted against midspan curvature in the plane of bending at the start of local buckling in Fig. 26. The points on this figure are taken from Table 4, and tests LB-13, LB-20, and LB-22 have been omitted because of either double curvature deformations (Fig. 20 and 21 for LB-13 and LB-20) or large movement of the support (Fig. 22 for LB-22). The points in Fig. 26 are still quite scattered, but it can be seen that local buckling occurred for most of the tests in a

curvature range of 8 to 12 ϕ_y . The average curvature for these tests is 11.5 ϕ_y .

One additional set of data is available for the local buckling phenomenon: In Table 4 are listed the measured maximum strains at a point one inch from the tip of the compression flange (Fig. 9) at the load point before the first observation start of local buckling. The strains are marked ϵ_c in this table, and they are also given in non-dimensionalized form, ϵ_c/ϵ_y , where ϵ_y is the strain at the theoretical start of yielding. These data too exhibit a lack of regularity, and they only show that local buckling started after strains ranging from 12 to 23 times the strain ϵ_y .

The apparent random scatter of the deformations at the start of local buckling would seem to be quite disturbing. One would expect that for the very similar conditions and remarkably similar performances of the beams, local buckling should have occurred in a less random manner.

Upon closer examination, this great variation can be attributed to various factors:

- (1) Local buckling was observed visually. The start of local buckling could have occurred before the points marked B in Figs. 10 to 19. All that is definitely known is that local buckling was present at this load point, and that it was not present at the point before this. Since in many cases the range between these two points amounts to 2 or even $3 \phi_y$, a great deal of this scatter would have been eliminated by a closer spacing of the deflection increments in the tests.
- (2) Local buckling did not necessarily occur directly at the center of the critical segment where the readings of deformation were taken. This would also account for some of the observed scatter.
- (3) Local buckling is dependent on the lateral buckling deformations. These in turn are a function of the initial crookedness of the compression flange. In most instances lateral

buckling occurred in the expected manner (see curves in Figs. 20 - 22). However, in at least two instances lateral buckling resulted in double curvature deformation (see curves for LB-13 and LB-20 in Figs. 20 and 21). Thus the initial state of the member can also be expected to play a role in final occurrence of local buckling.

4. SUMMARY AND CONCLUSIONS

4.1 PLASTIC HINGE BEHAVIOR

The M- θ curves for all the 14 tests performed in this experimental program show (see Figs. 11 - 15) that each beam delivered a plastic hinge with a certain amount of rotation capacity. This rotation capacity varied to some extent; however, this variation could not be conclusively attributed to the variations of any of the varied test parameters, which consisted essentially of the variation of the purlin stiffnesses. Unloading was in most cases triggered by local buckling, but this was never catastrophic. Each specimen can be considered to have exhibited a rotation capacity of at least 10 θ_y before

serious unloading occurred.

The question of whether the rotation capacity is sufficient cannot of course be directly answered since each structure will have different inelastic rotation requirements. However, a study of the possible extreme rotation requirements in commonly used steel structures has been performed⁽⁸⁾. An examination of the results of this study has shown that the maximum rotation requirements for hinges occurring between panel points in all the structures which were investigated occurred in the windward rafter of the two-bay gabled frame which has been reproduced from Ref. 8 in Fig. 27. This hinge rotation requirement was 0.057 radians. In this comparison only hinges forming between panel points have been considered, since this is the situation most resembling the test conditions. At the panel points the moment gradient is usually quite large, and it is therefore necessary to restrict the comparison to cases where the hinge forms at regions of nearly uniform moment.

The rotation capacity of the test beams can be computed as the sum of the two angles at the ends of the critical span (θ in Fig. 1). Since the moment, as well as the curvature

were uniform across this span, the end slope is equal to $\theta = \frac{\phi L}{2}$. The total inelastic rotation is

$$H = \phi_y L \left[\phi / \phi_y - 1 \right] \quad (5)$$

The values of H for each test are listed in Table 4. These values of H represent the situation at the onset of local buckling. It can be seen that these rotations are well above the maximum requirements.

4.2 INFLUENCE OF THE VARIATION OF THE TEST PARAMETERS

The experiments described in this report were designed to furnish information on the inelastic behavior of braced beams. One of the questions to be investigated was the minimum stiffness of the lateral bracing. The results of these experiments indicate that the bracing need possess very little lateral stiffness as long as it is able to hold the compression flange in place at the braced point so that the member at this point is effectively prevented from lateral deflection. As the M- ϕ curve for test LB-15 shows, no added lateral stiffness of the purlin is required. The presence of purlins of greatly varying stiffness (purlin slenderness ratio of 142 for LB-12 to 279 for test LB-19, Table 1) did not noticeably influence the results. The results of the tests were also not influenced by the method

of loading (compression flange and tension flange loading, tests Lb-18 and Lb-13) or by the method of attaching the purlins. Nor did it seem to matter that in test P-9 stiffeners were not provided over the whole depth of the section.

The tests have revealed that the one important and indispensable function of the lateral bracing is to prevent the compression flange from moving laterally at the point of bracing. Any arrangement of lateral bracing which is able to do this would seem satisfactory. However, the bracing which is provided must be assured to perform this function. The area of the bracing member need be only nominal as long as it can be assumed that the bracing is able to take the small axial forces in tension. Since in all frames except the outer one, bracing will extend in both directions from the main beam, behavior of this type can be reasonably expected. In outside frames (simulated by tests LB-22 and P-10) the bracing must take these forces in compression, and therefore a larger bracing member is required.

4.3 ADDITIONAL RECOMMENDED RESEARCH

In this report no theoretical solution to the bracing

problem has been presented, and the limited number of tests do not warrant the expostulation of a definite set of design rules. Theoretical work is now underway, and it is hoped that the reflections on the behavior of braced beams presented herein will be of use in formulating a mathematical model of a wide-flange beam in the post-buckling range. It is especially important to determine reliably the onset of local buckling. Since the beams do not fail rapidly after local buckling, it would also seem profitable to investigate the post-local buckling behavior of yielded plates. It is desirable to investigate the following additional aspects of the problem of bracing requirements experimentally:

- (1) Since it is of paramount importance that the bracing be able to prevent the compression flange of the braced point from lateral motion, it is desirable to know whether purlins which form a plastic hinge at the same time as the braced beam can adequately perform this function. This problem should be investigated through testing several beam-purlin assemblies by also loading the purlin members.

- (2) The results of the experiments presented here would lead one to assume that only the compression flange must be braced. This question is not conclusively answered by these tests, and it is recommended that a test be performed which is in all aspects similar to that LB-15, except that the knife-edge guides act only on the compression flange at the braced point.
- (3) It is desirable to possess reliable measurements on the axial force in the purlins, and therefore it is suggested to perform a test identical to LB-18, except that the purlins be replaced by round tension bars or wires which are provided with strain gages to measure the axial force.
- (4) The results of test P-9 showed no noticeable effect from using a stiffener only over part of the web at the bracing point. From reasons of economy it would be desirable to find out if the complete absence of a stiffener

would significantly change the behavior. Therefore it is recommended that a test similar to P-9 be performed, but that there be no stiffeners at all at the bracing points.

4.4 INFLUENCE OF THE TEST RESULTS ON DESIGN

It is obvious that because of the lack of an adequate theory and the limited number of tests it is not possible to formulate design rules from the material presented in this report. However, these experiments can serve as a guide for checking the adequacy of bracing. There is no question about the adequacy of the bracing in the tests reported, and therefore bracing which is similar to it, should also perform adequately. Thus bracing which fulfills the following requirements should be satisfactory in plastic design:

- (1) Lateral bracing spaced so that a brace is provided at the plastic hinge and at a distance of $40r_y$ in both directions away from the plastic hinge.

- (2) The bracing members are designed elastically such that no plastic hinge exists in them at the time of failure of the braced member.
- (3) Purlin depth to beam depth ratio is at most 3.5.
- (4) Purlins are attached by welding or bolting to the compression flange of the braced beam.
- (5) A vertical stiffener is provided for at least half the depth of the web at the bracing point.
- (6) The weak axis slenderness ratio of the purlins is less than 200 if purlins extend in both directions from the braced beam, or less than 100 if purlins extend in one direction only.

5. ACKNOWLEDGEMENTS

This study is part of the general investigation "Welded Continuous Frames and Their Components" currently being carried out at Fritz Engineering Laboratory, Lehigh University, under the direction of Dr. L. S. Beedle. The investigation is sponsored jointly by the Welding Research Council and the Department of the Navy, with funds furnished by the American Iron and Steel Institute, American Institute of Steel Construction, Office of Naval Research, Bureau of Ships and Bureau of Yards and Docks.

The suggestions arising from discussions with members of the Lehigh Project Subcommittee of the Welding Research Council are sincerely acknowledged.

The authors express their appreciation to Messrs. Y. Fukumoto and J. Prasad for their assistance in the experiments, to Mr. K. Harpel, Laboratory Foreman, and his assistant for their effort in the preparation of the tests, to Miss V. Austin for typing the manuscript, and to Messrs. R. Sopko and J. Szilagyi for preparation of the drawings.

6. NOMENCLATURE

M	=	Bending moment
M_p	=	Full plastic moment = $\sigma_y \cdot Z$
Z	=	Plastic modulus
L_{cr}	=	Length of span under consideration
L_{adj}	=	Length of adjacent span
l	=	Length of purlins
d	=	Overall depth of a section
b	=	Flange width
t	=	Flange thickness
w	=	Web thickness
r_y	=	Radius of gyration about the y-y axis
ϕ	=	Curvature
ϕ_y	=	Curvature at the start of yielding
σ_y	=	Yield stress
E	=	Modulus of elasticity
ksi	=	Kips per square inch

7. TABLES AND FIGURES

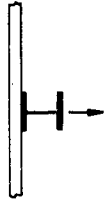
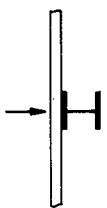

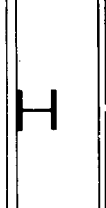
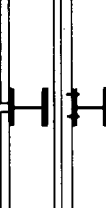
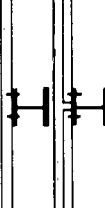

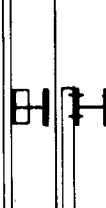

TEST NO.	BEAM			PURLINS				PURPOSE	DETAILS OF PURLIN ATTACHMENT
	SIZE	SPAN LENGTH		SIZE	LENGTH				
		CRITICAL	ADJACENT		λ_d	λ_{ry}	INCHES		
LB-12	10W25	40 r_y	40 r_y	417.7	21	142	84	Effect of purlin size	
LB-13	"	"	"	315.7	28	159	"	"	
LB-14	"	"	"	M2362	32	206	"	"	
LB-18	"	"	"	315.7	28	159	"	Effect of purlin slenderness	
LB-19	"	"	"	"	49.3	279	148	"	
LB-20	"	"	"	"	38.7	219	116	"	
LB-22	"	"	"	"	18.7	105	56	Effect of purlins on one side only (welded)	
P-3	8B13	"	"	M2362	28	180	73.5	Effect of beam size and local buckling	
P-4	"	"	60 r_y	"	"	"	"	Effect of length of adjacent spans	
P-6	10W25	"	40 r_y	315.7	"	159	84	Effect of beam-to-purlin connection — discontinuous purlins welded	
P-7	"	"	"	"	"	"	"	Effect of beam-to-purlin connection — continuous purlins bolted	
P-8	"	"	"	"	"	"	"	Effect of beam-to-purlin connection — discontinuous purlins bolted	
P-9	"	"	"	"	"	"	"	Effect of half stiffeners	
P-10	"	"	"	"	18.7	105	56	Effect of purlins on one side only (bolted)	

Table 1 Outline of Test Program

TEST NO.	SECTION	σ_{yF} ksi	σ_{yW} ksi	M_{PI} kip-in	M_{P2} kip-in
LB-12	10 WF 25	34.0	38.8	1011	1095
LB-13	"	"	"	1012	"
LB-14	"	"	"	1005	"
LB-18	"	"	"	994	"
LB-19	"	"	"	979	"
LB-20	"	"	"	979	"
LB-22	"	38.8	43.8	1156	1145
P-3	8B13	38.5	47.7	482	466
P-4	"	"	"	488	"
P-6	10 WF 25	38.8	43.8	1130	1145
P-7	"	"	"	1130	"
P-8	"	"	"	1127	"
P-9	"	"	"	1137	"
P-10	"	"	"	1140	"

Table 2 Material Properties

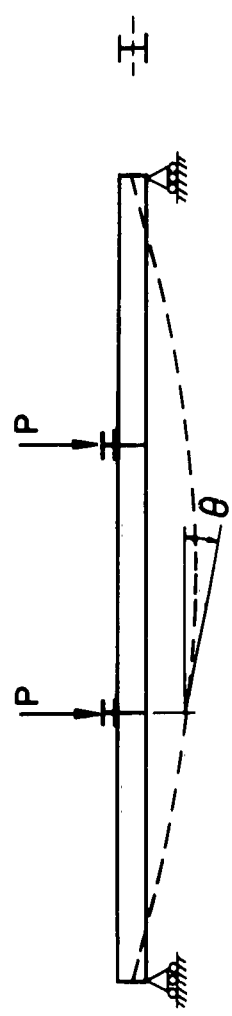
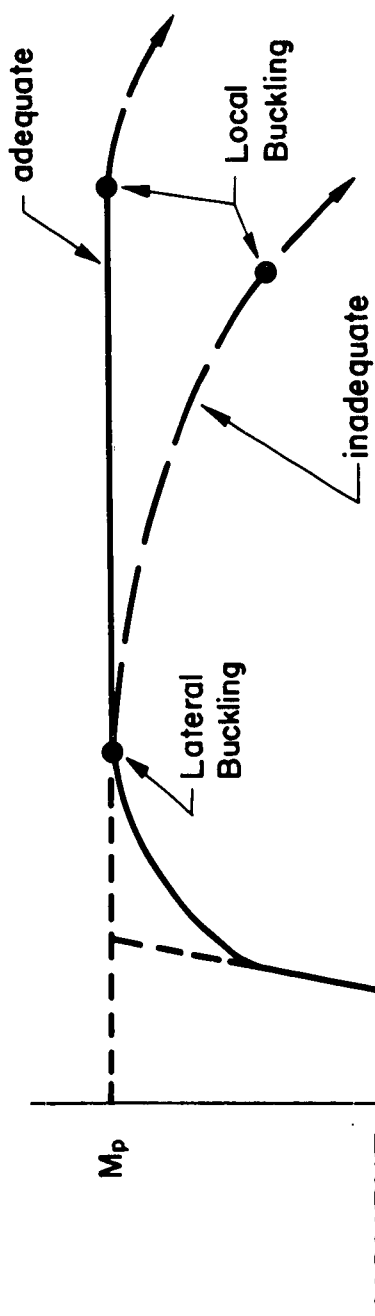
SECTION	AREA OF SECTION A , sq.in.	FLANGE WIDTH b , in.	DEPTH OF SECTION d , in.	WEB THICKNESS w , in.	FLANGE THICKNESS t , in.	$\frac{d}{w}$	$\frac{b}{t}$	MOMENT OF INERTIA about x-axis I_x , in. ⁴	RADIUS OF GYRATION about y-axis r_y , in.
10WF25	7.35	5.762	10.08	0.252	0.430	40.0	13.4	133.2	1.31
8BI3	3.83	4.00	8.00	0.230	0.254	34.8	15.75	39.5	0.83
4I7.7	2.21	2.66	4.00	0.190	0.293	21.0	10.0	6.0	0.59
3I5.7	1.64	2.33	3.00	0.170	0.260	17.6	9.0	2.9	0.52
M2362*	1.085	1.840	2.625	0.156	0.201	16.8	9.2	1.236	0.407

* Special section produced by Bethlehem Steel Co.

Table 3 Section Properties

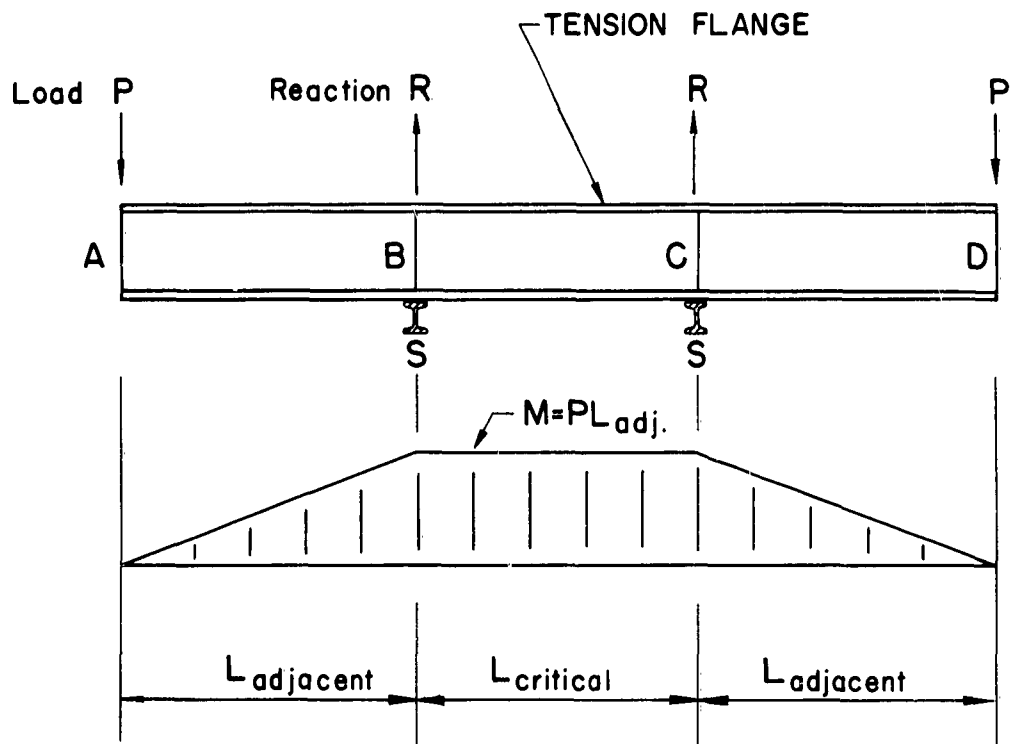
TEST NO.	ϕ/ϕ_y	$\frac{u_c}{L}$	$\frac{\beta}{L}$	$S_{ADJ.}$	S_{PURLIN}	S	ϵ_c	$\frac{\epsilon_c}{\epsilon_y}$	H
LB-15	12.8	0.0386	0.00363	0.121	0	0.121	0.022	19	0.16
LB-12	20.8	0.0262	0.00280	"	0.018	0.139	0.026	23	0.27
LB-13	9.9	0.0053	0.00044	"	0.011	0.132	0.014	12	0.12
LB-14	12.8	0.0264	0.00229	"	0.005	0.126	0.023	20	0.16
LB-18	12.3	0.0160	0.00132	"	0.011	0.132	0.014	12	0.16
LB-19	11.0	0.0174	0.00149	"	0.006	0.127	—	—	0.14
LB-20	7.2	0.0030	0.00029	"	0.008	0.129	—	—	0.09
LB-22	8.3	0.0267	0.00147	"	0.008	0.129	0.016	12	0.11
P-3	13.3	0.0241	0.00286	0.039	0.006	0.045	—	—	0.16
P-4	12.1	0.0141	0.00139	0.026	0.006	0.032	0.023	18	0.14
P-6	9.4	0.0193	0.00143	0.121	0.011	0.132	0.015	12	0.13
P-7	9.3	0.0158	0.00145	"	0.011	0.132	0.021	16	0.13
P-8	10.3	0.0222	0.00204	"	0.011	0.132	0.022	17	0.14
P-9	8.1	0.0162	0.00141	"	0.011	0.132	0.017	13	0.11
P-10	7.5	0.0160	0.00132	"	0.008	0.129	0.018	14	0.10

Table 4 Test Results



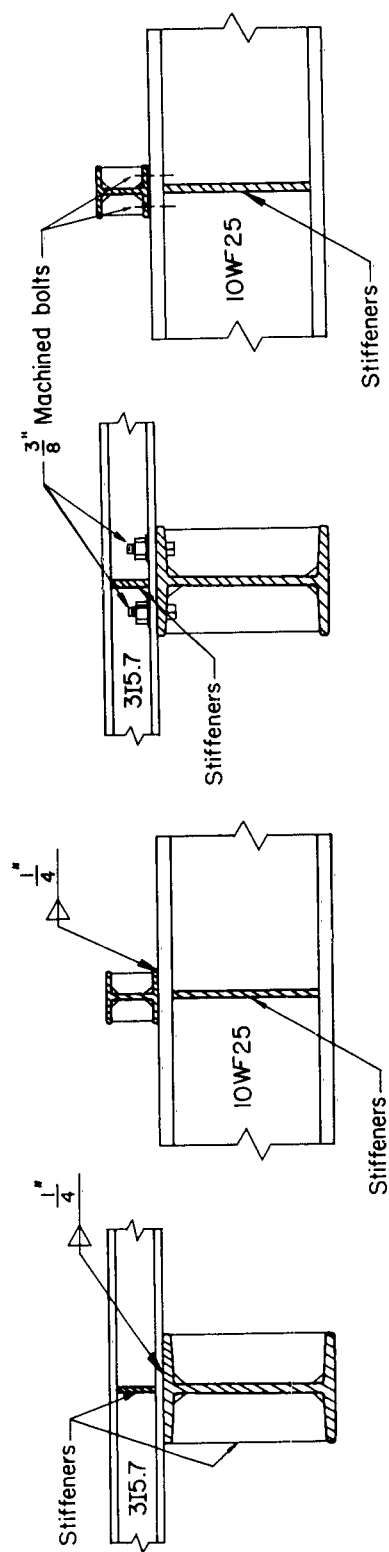
ROTATION θ

Fig. 1 Typical M- θ Relationships



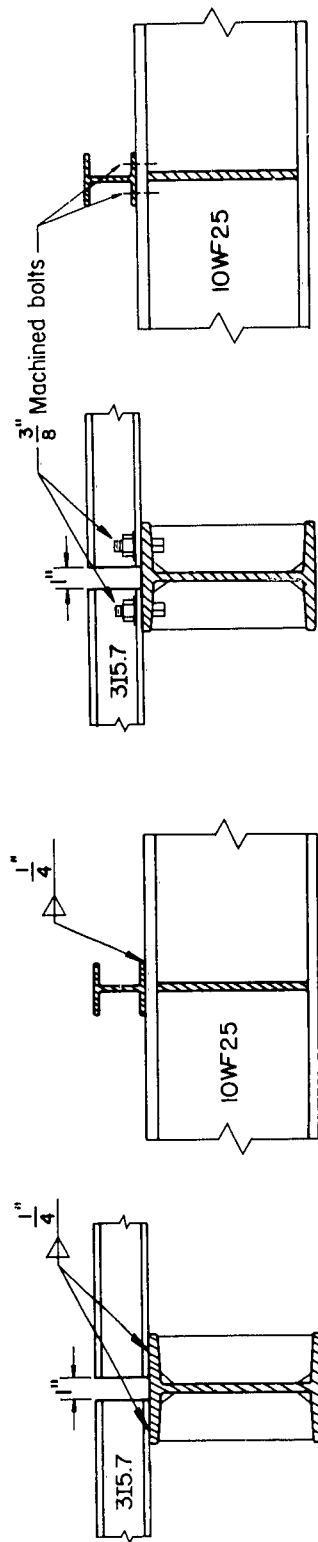
R - POINTS OF LOADING FOR LB-12,13,14 AND P-6,8
 S - POINTS OF LOADING FOR LB-18,19,20,22 AND P-3,4,7,9,10
 A, B, C, D, POSITIONS OF LATERAL SUPPORT

Fig. 2 Loading System



(a) WELDED CONTINUOUS CONNECTION (LB-18 & OTHERS)

(c) BOLTED CONTINUOUS CONNECTION (P-7)



(b) WELDED DISCONTINUOUS CONNECTION (P-6)

(d) BOLTED DISCONTINUOUS CONNECTION (P-8)

Fig. 3 Beam-to-Purlin Connections

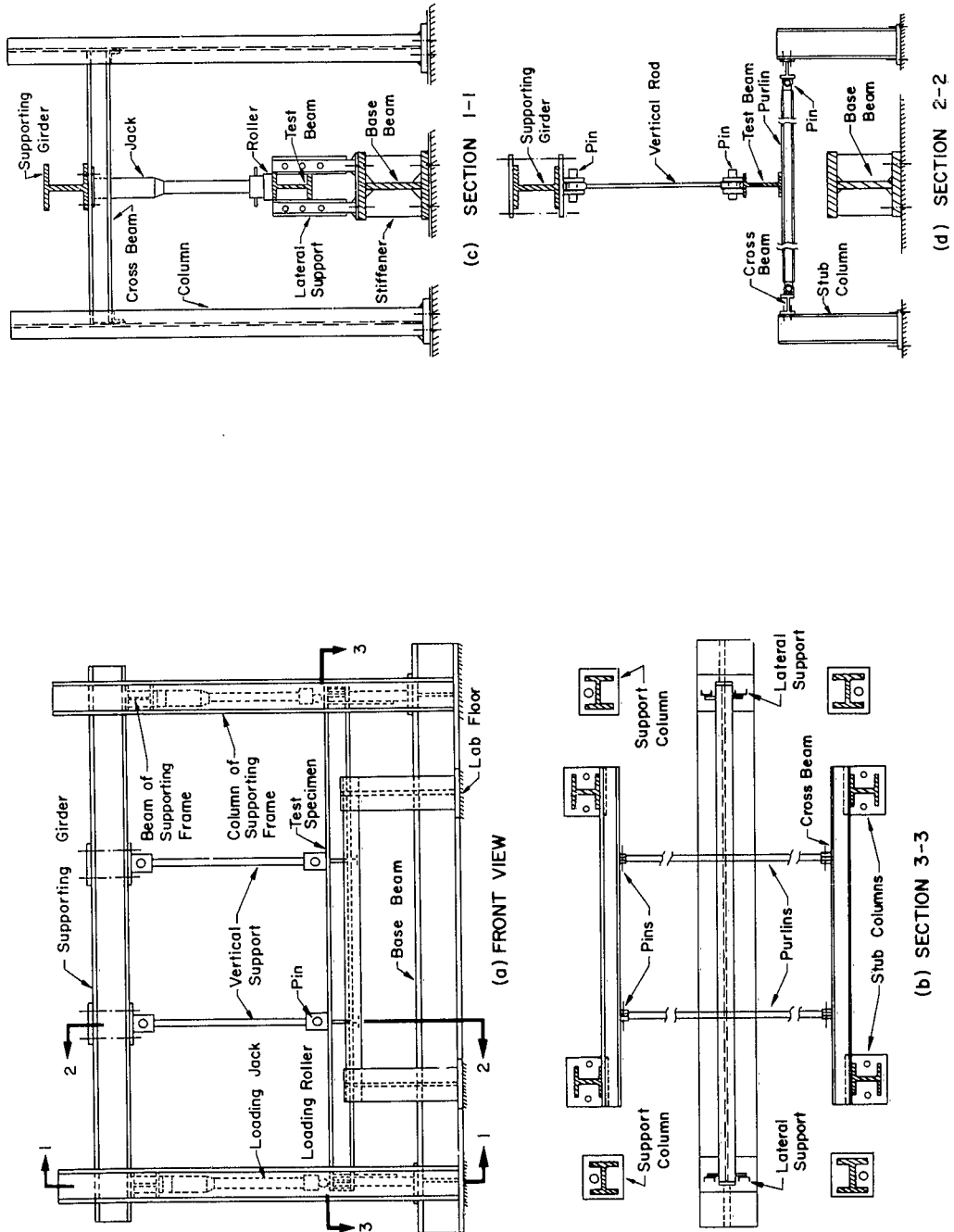


Fig. 4
Test Set-Up

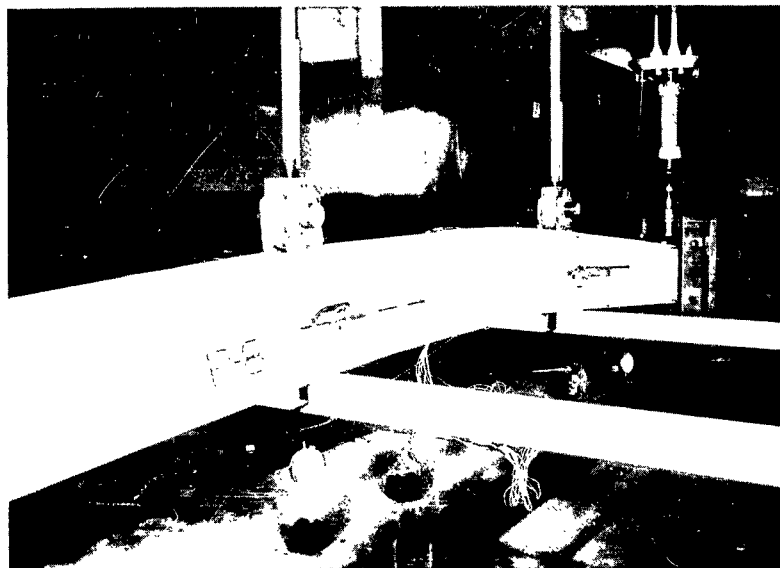


Fig. 5 Tension Flange Loading

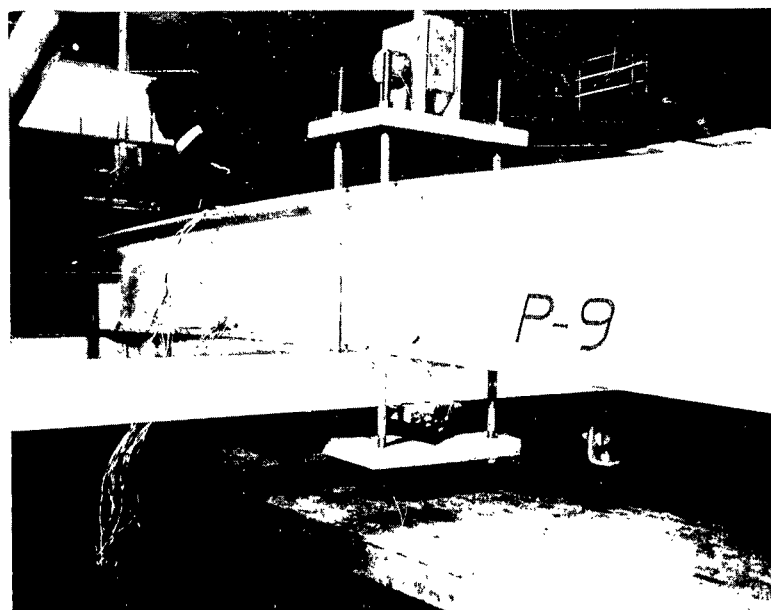


Fig. 6 Compression Flange Loading

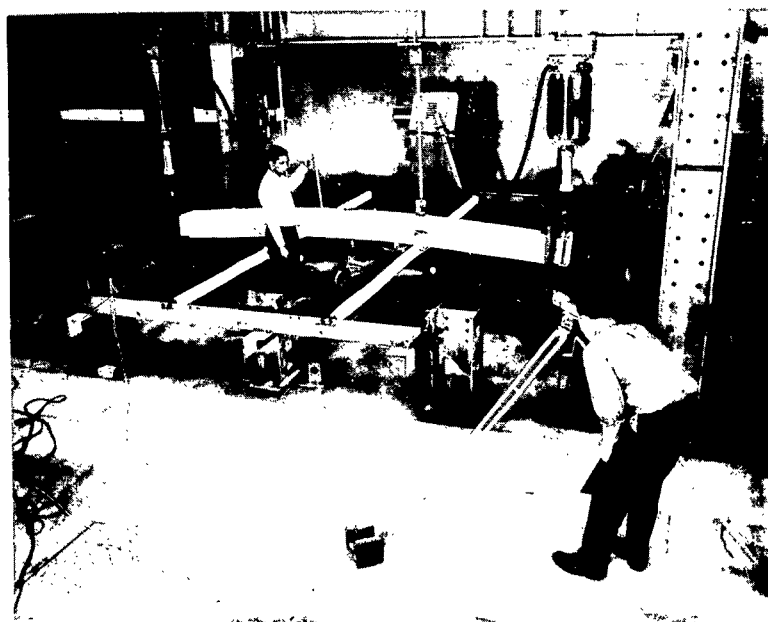
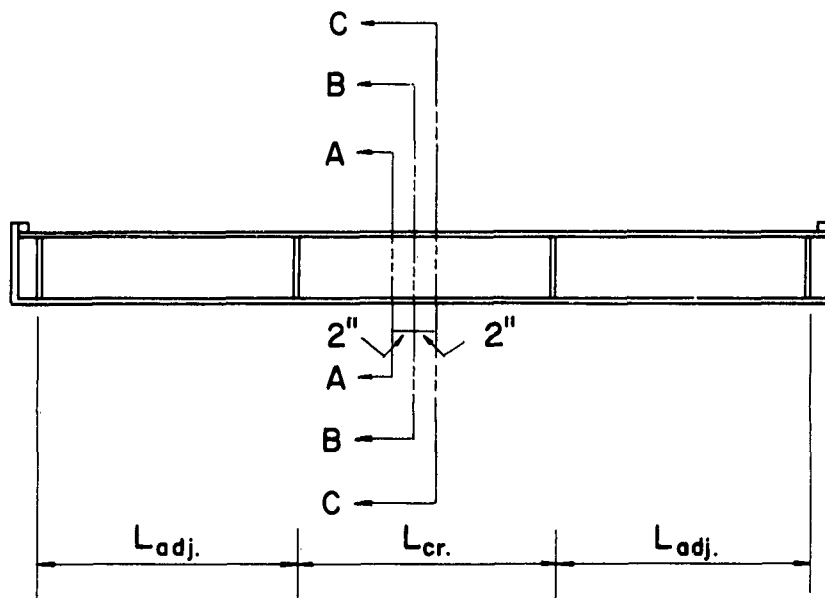
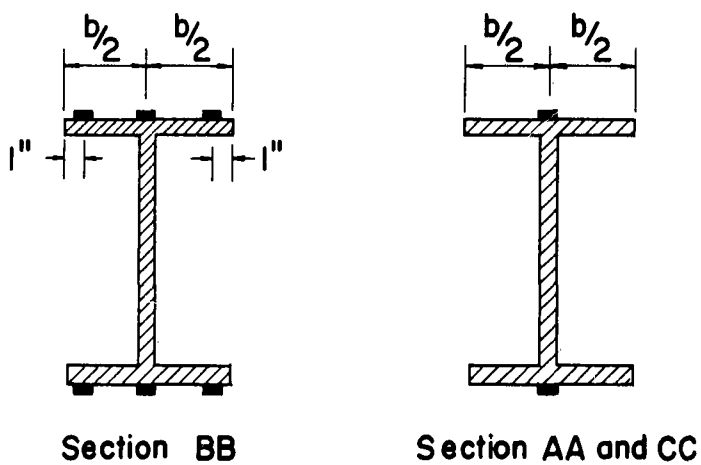


Fig. 7 Test in Progress



(a) SECTIONS WHERE STRAIN GAGES ARE ATTACHED



(b) LOCATION OF STRAIN GAGES

Fig. 8

Arrangement of Strain Gages

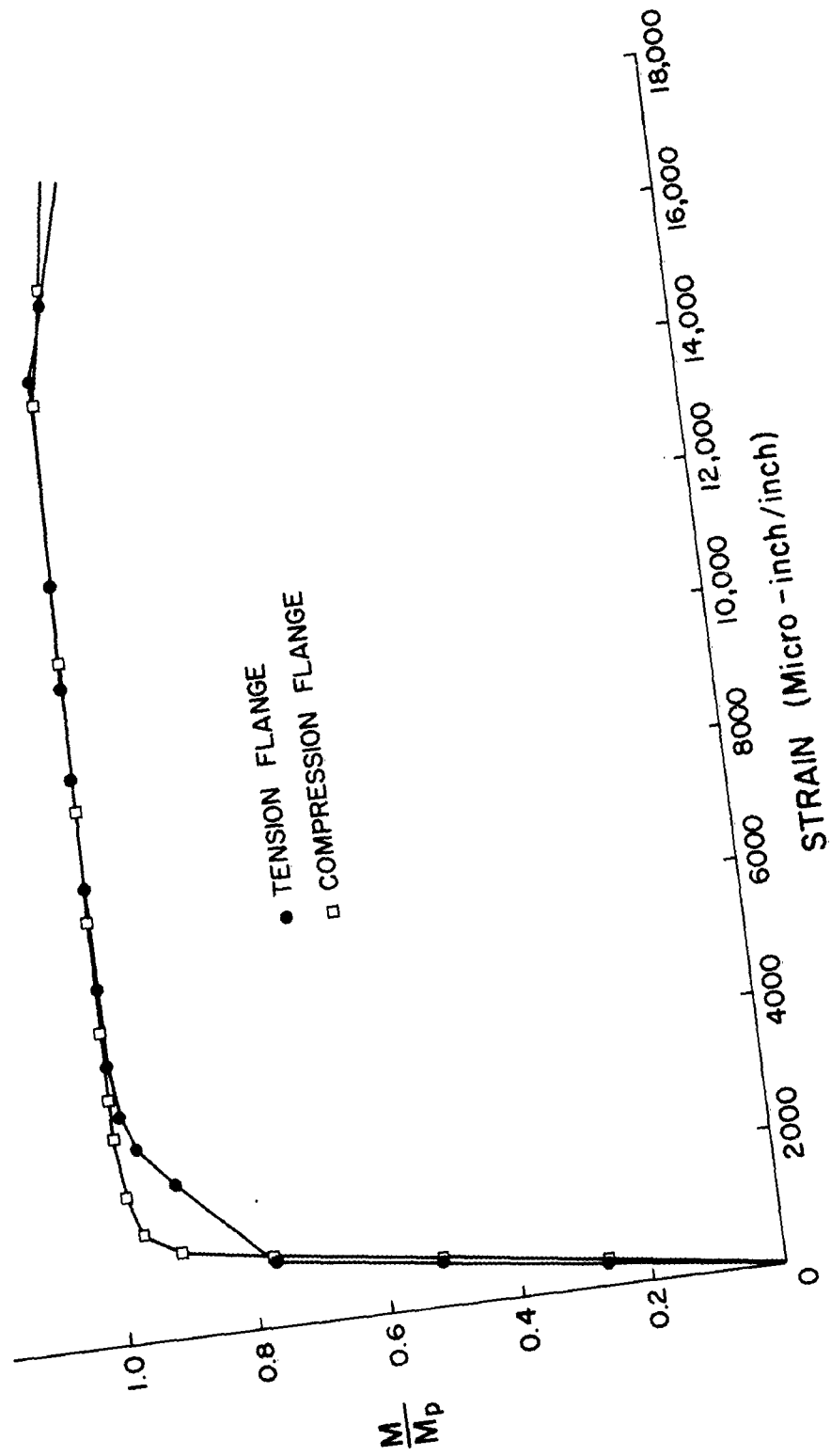


Fig. 9 Moment-versus-Strain at the Beam Center

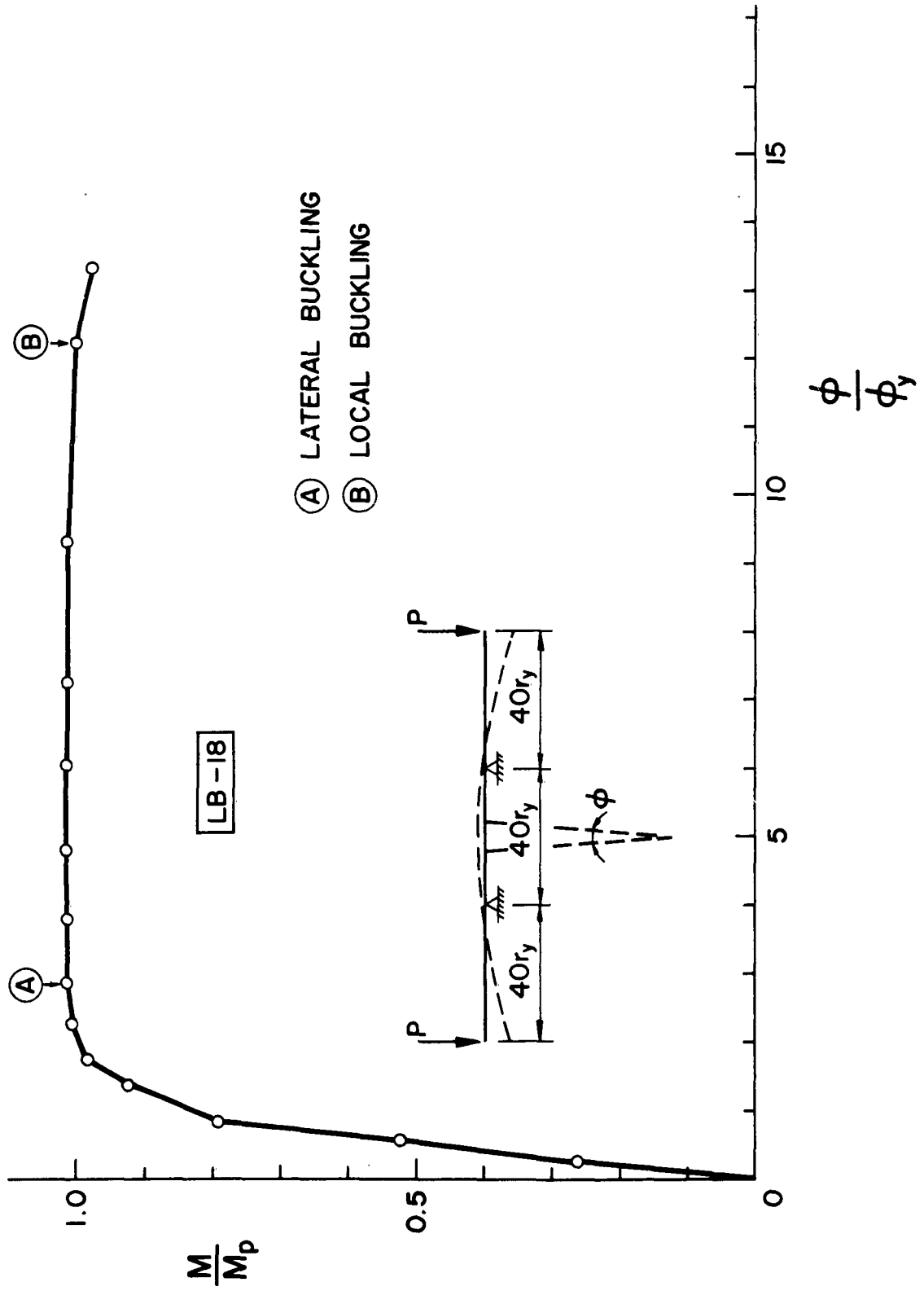
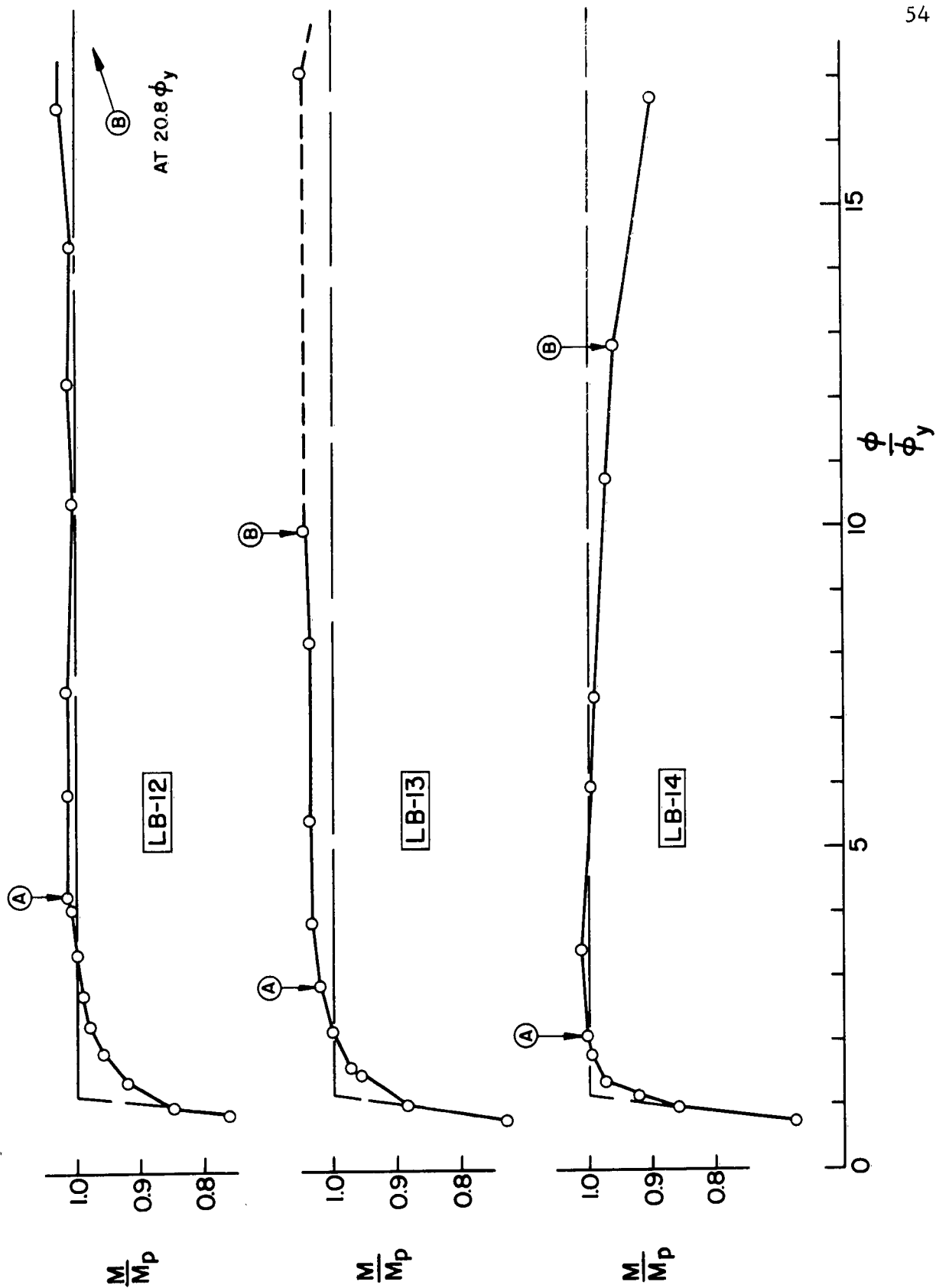
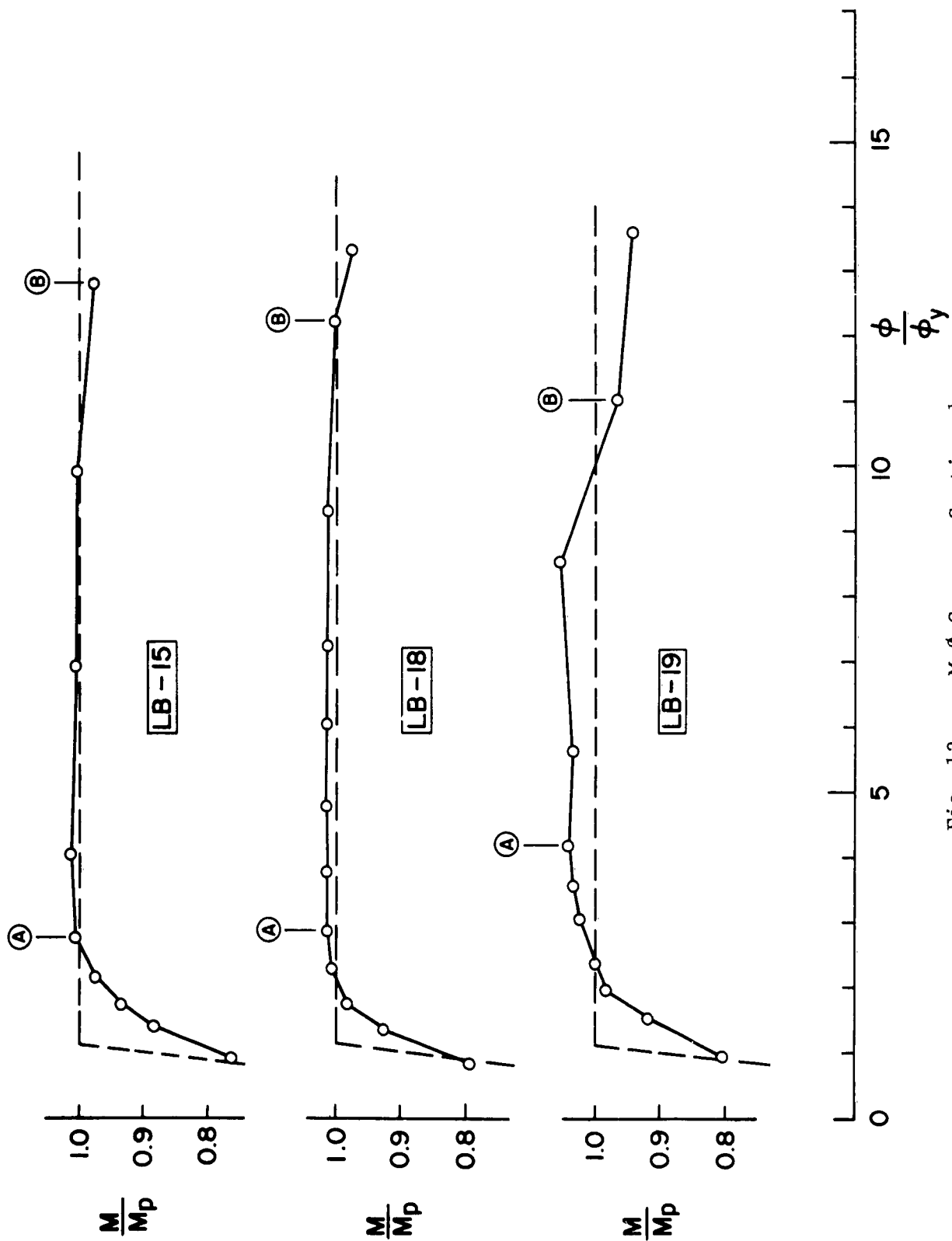


Fig. 10 Typical Moment-Curvature Relations

Fig. 11 M- ϕ Curves

Fig. 12 M- ϕ Curves, Continued

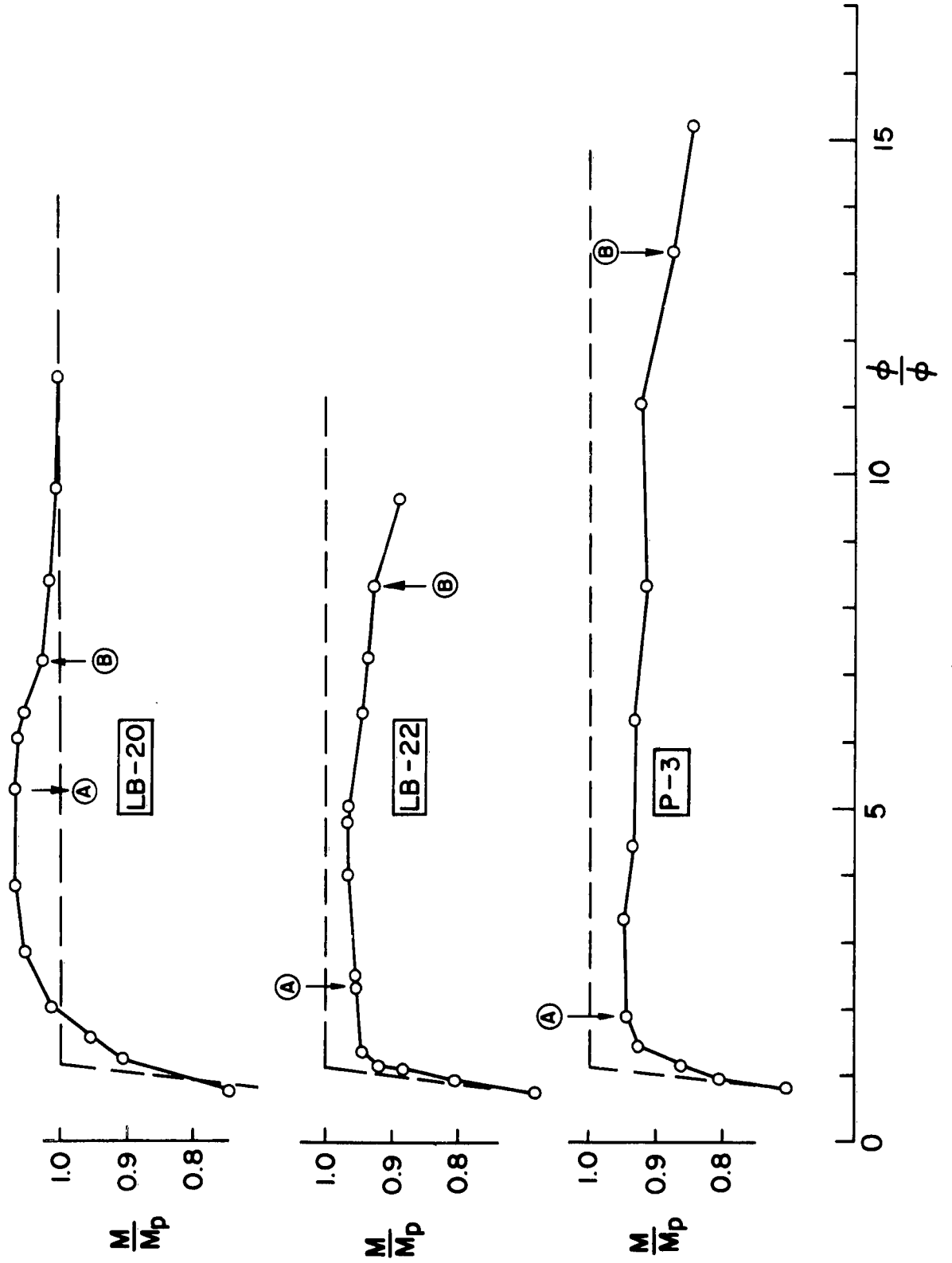
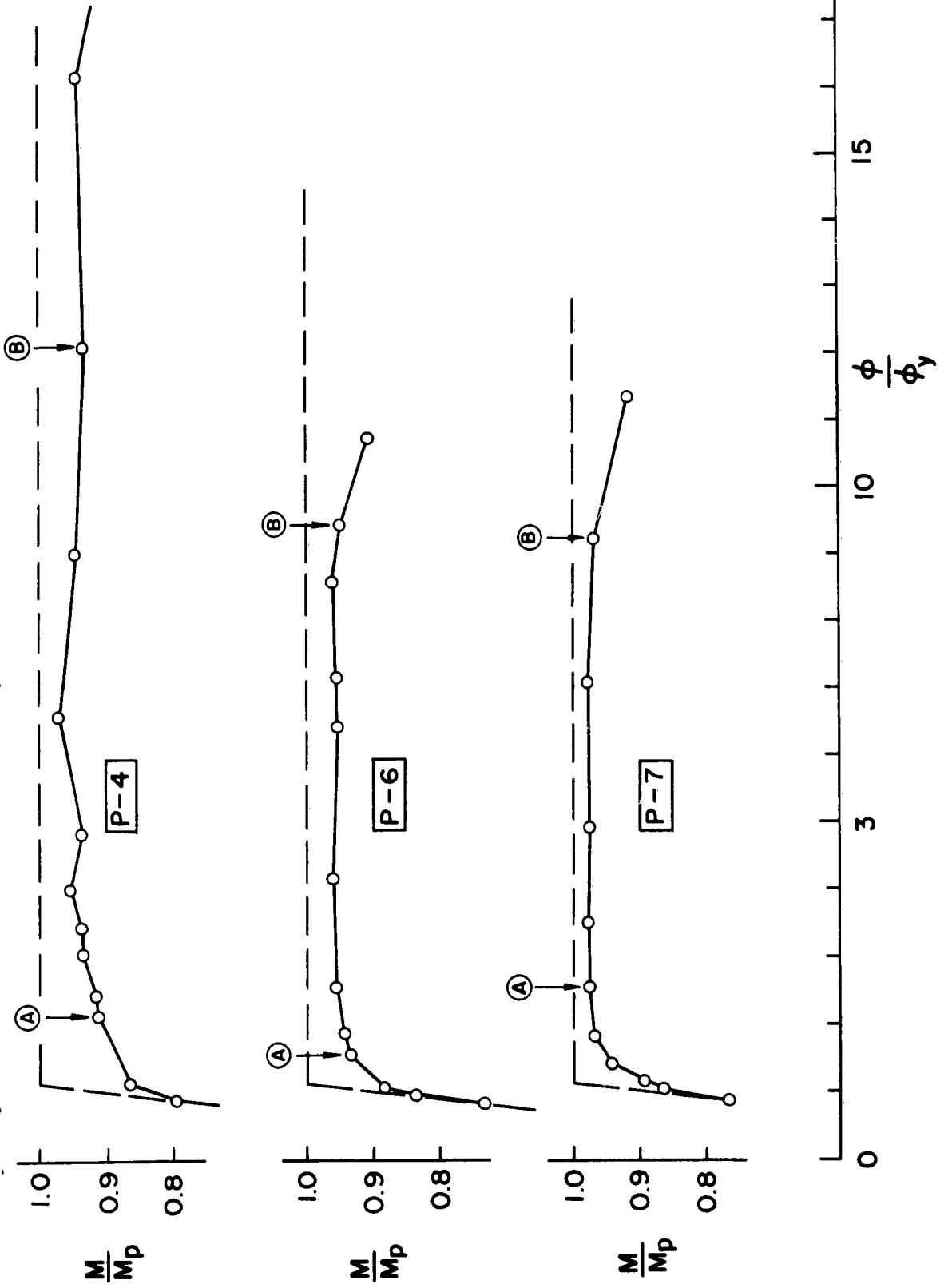
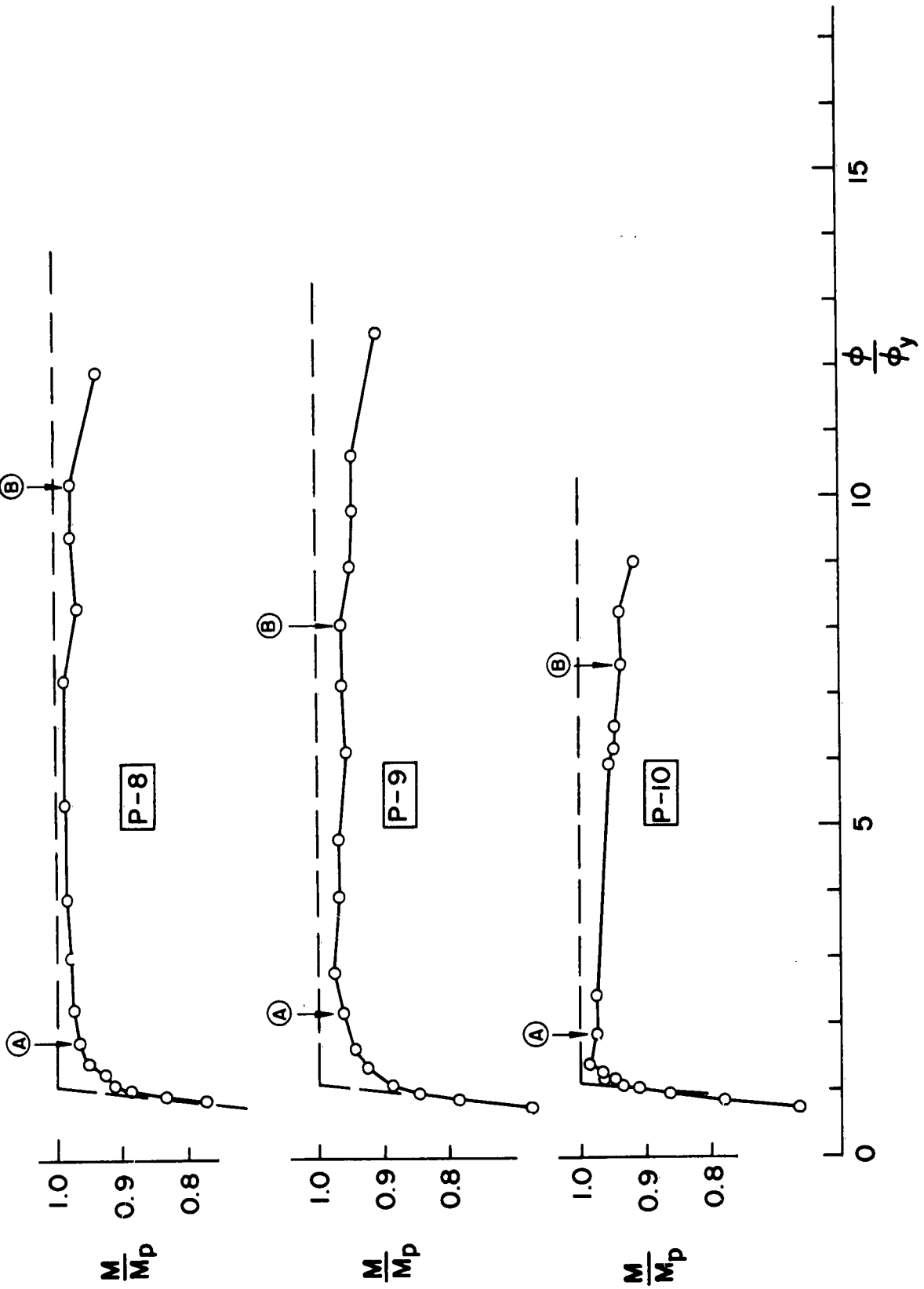


Fig. 13 M- ϕ Curves, Continued

Fig. 14 M- ϕ Curves, Continued

Fig. 15 M- ϕ Curves, Continued

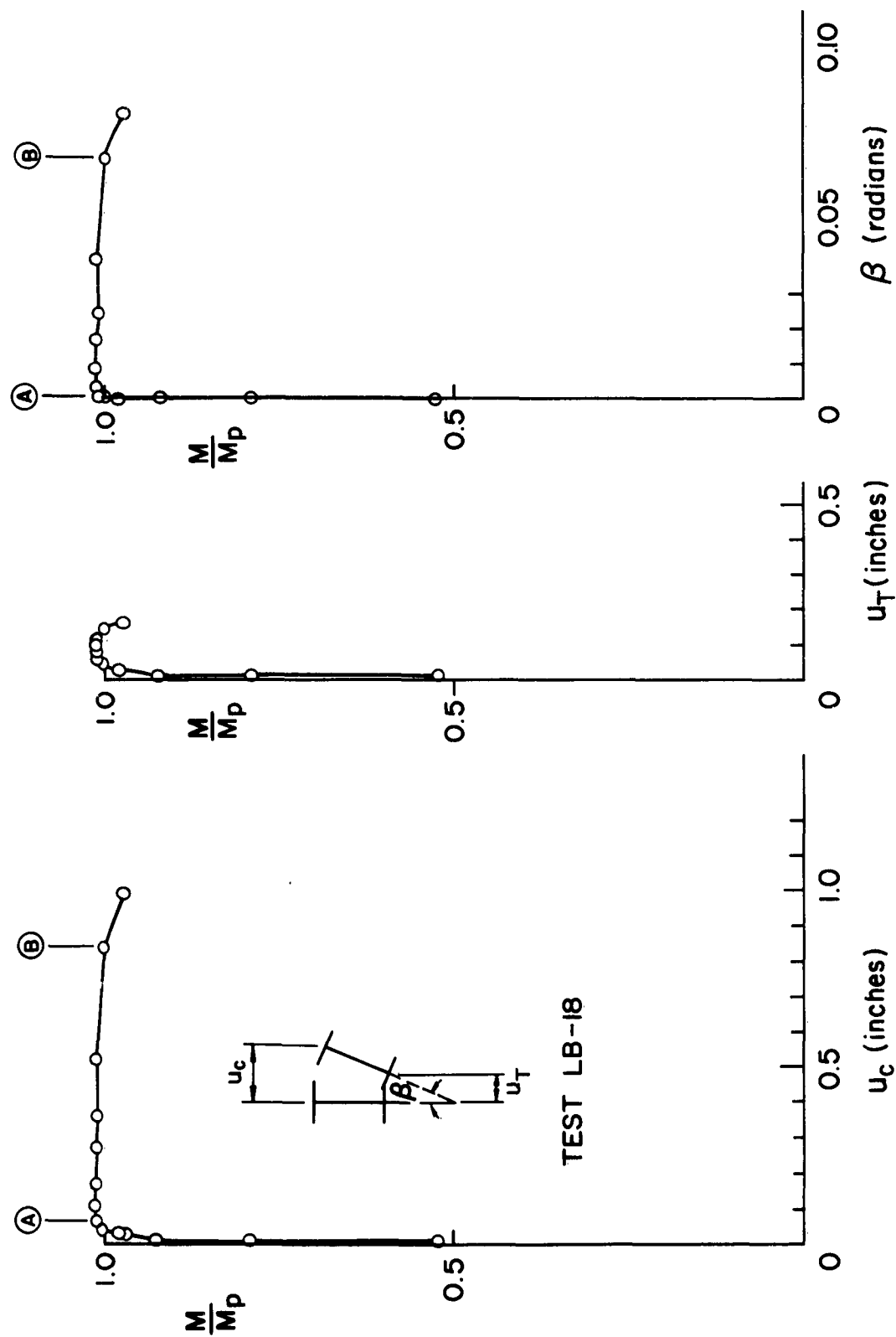


Fig. 16 Typical Moment-versus-Lateral Deformation Relations

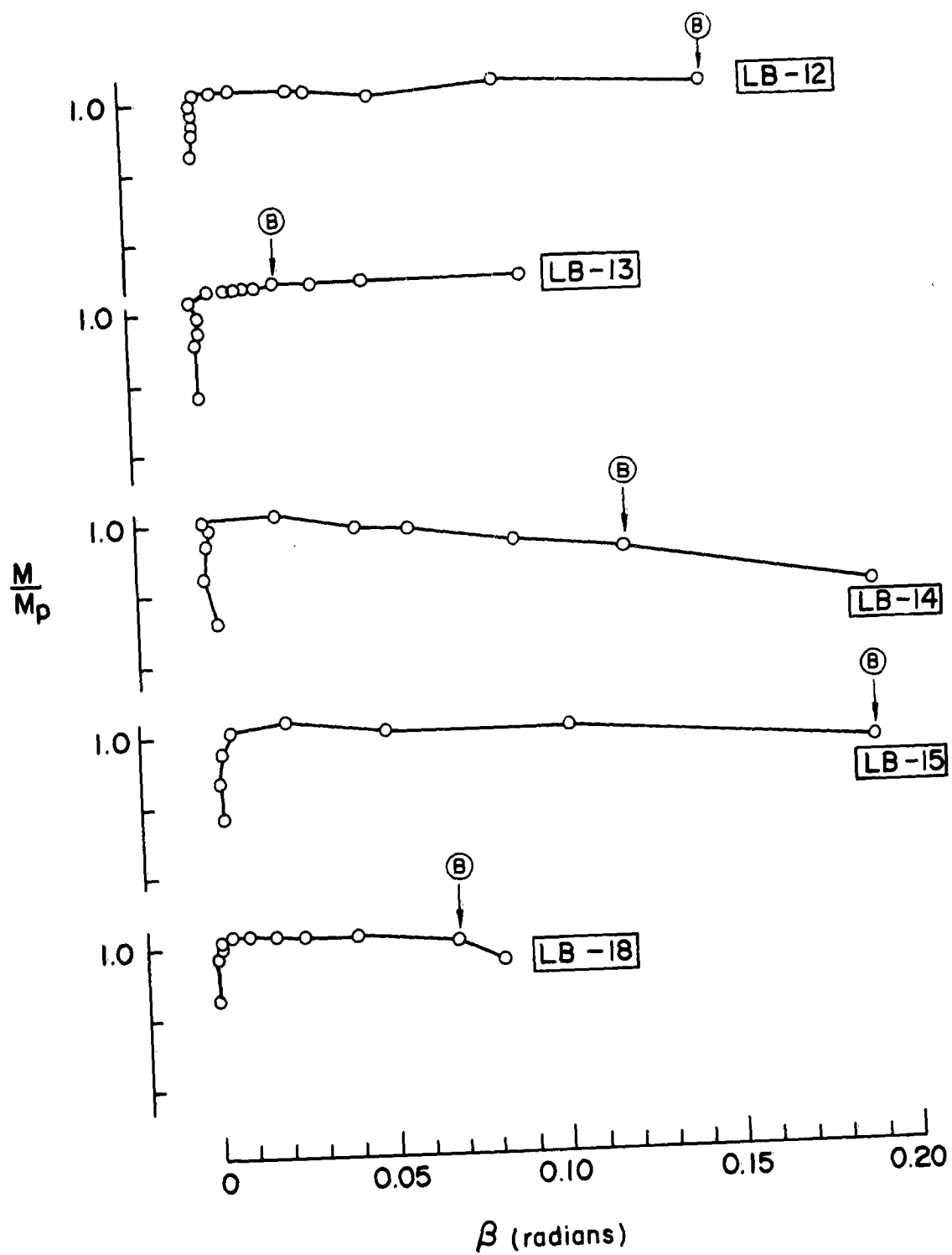


Fig. 17 M- β Curves

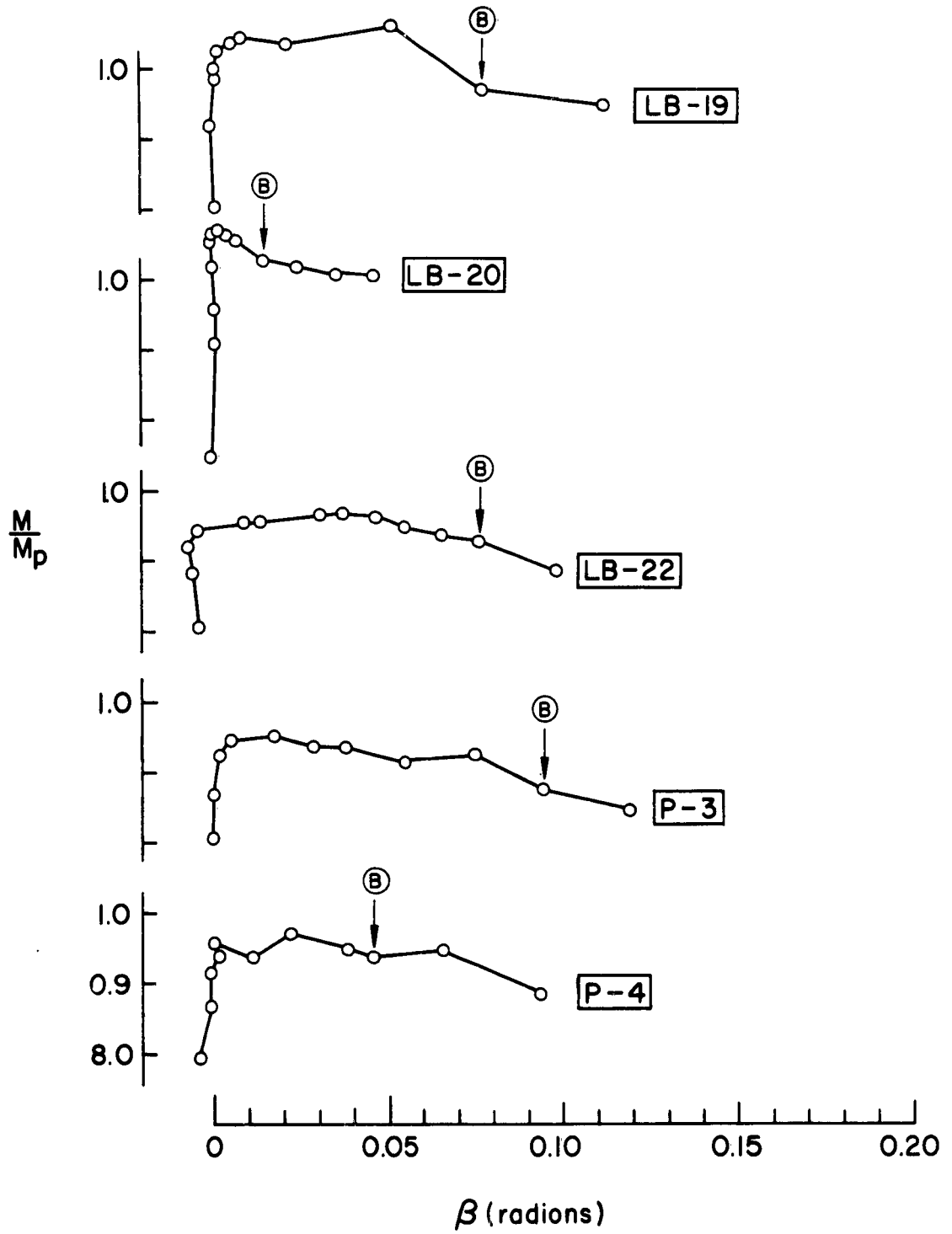


Fig. 18

M- β Curves, Continued

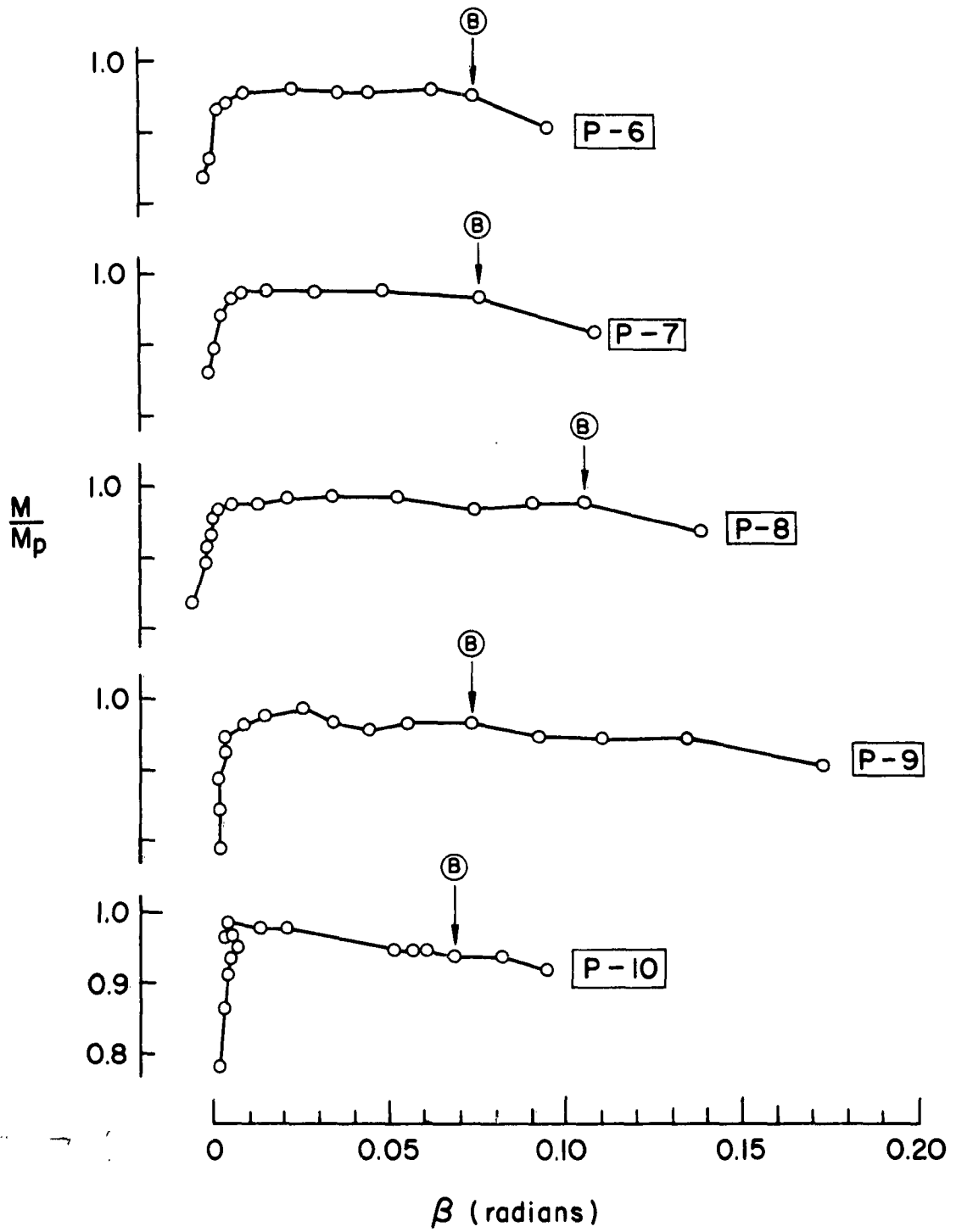


Fig. 19 $M-\beta$ Curves, Continued

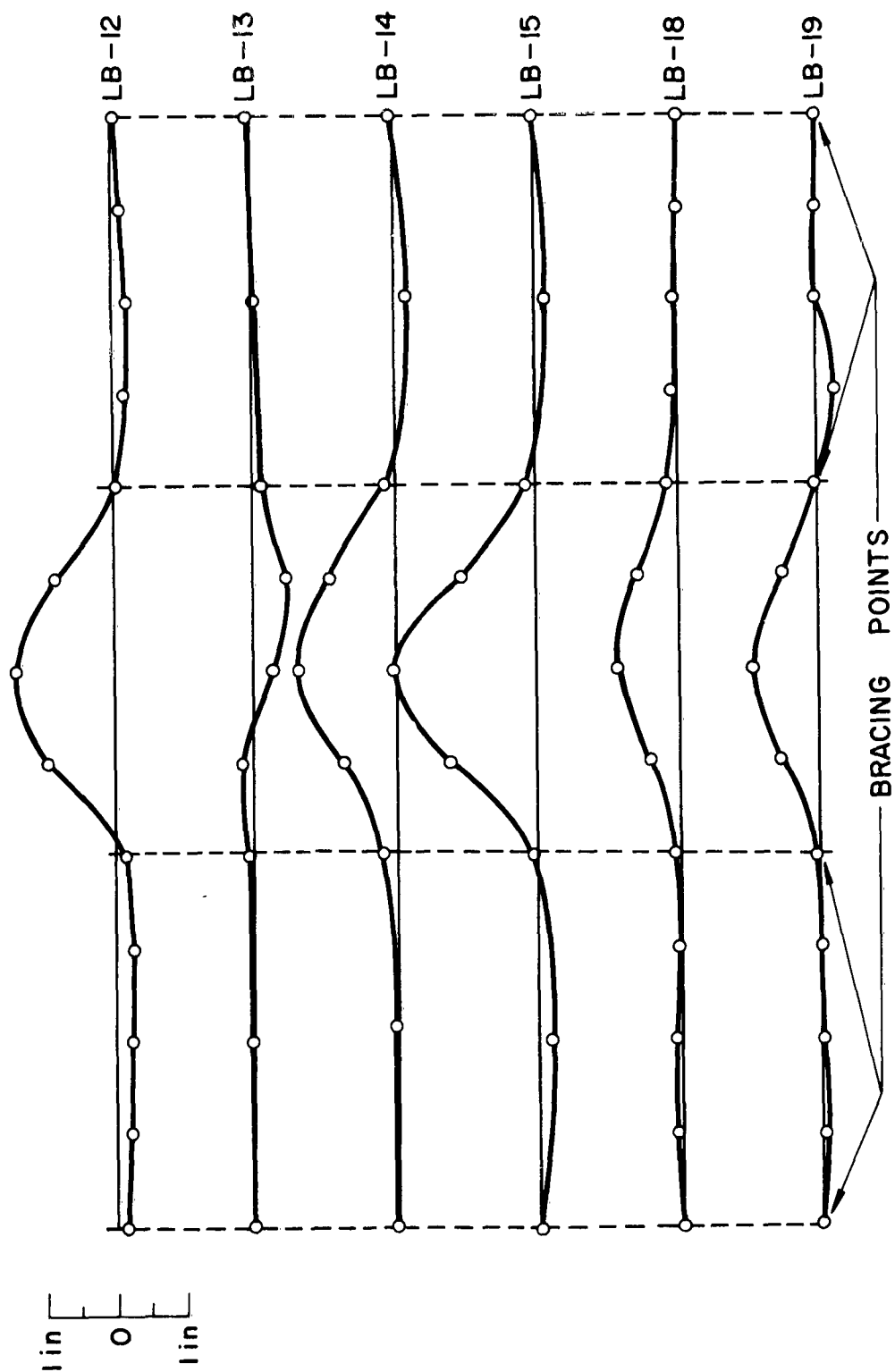


Fig. 20 Deflected Shapes of the Compression Flange

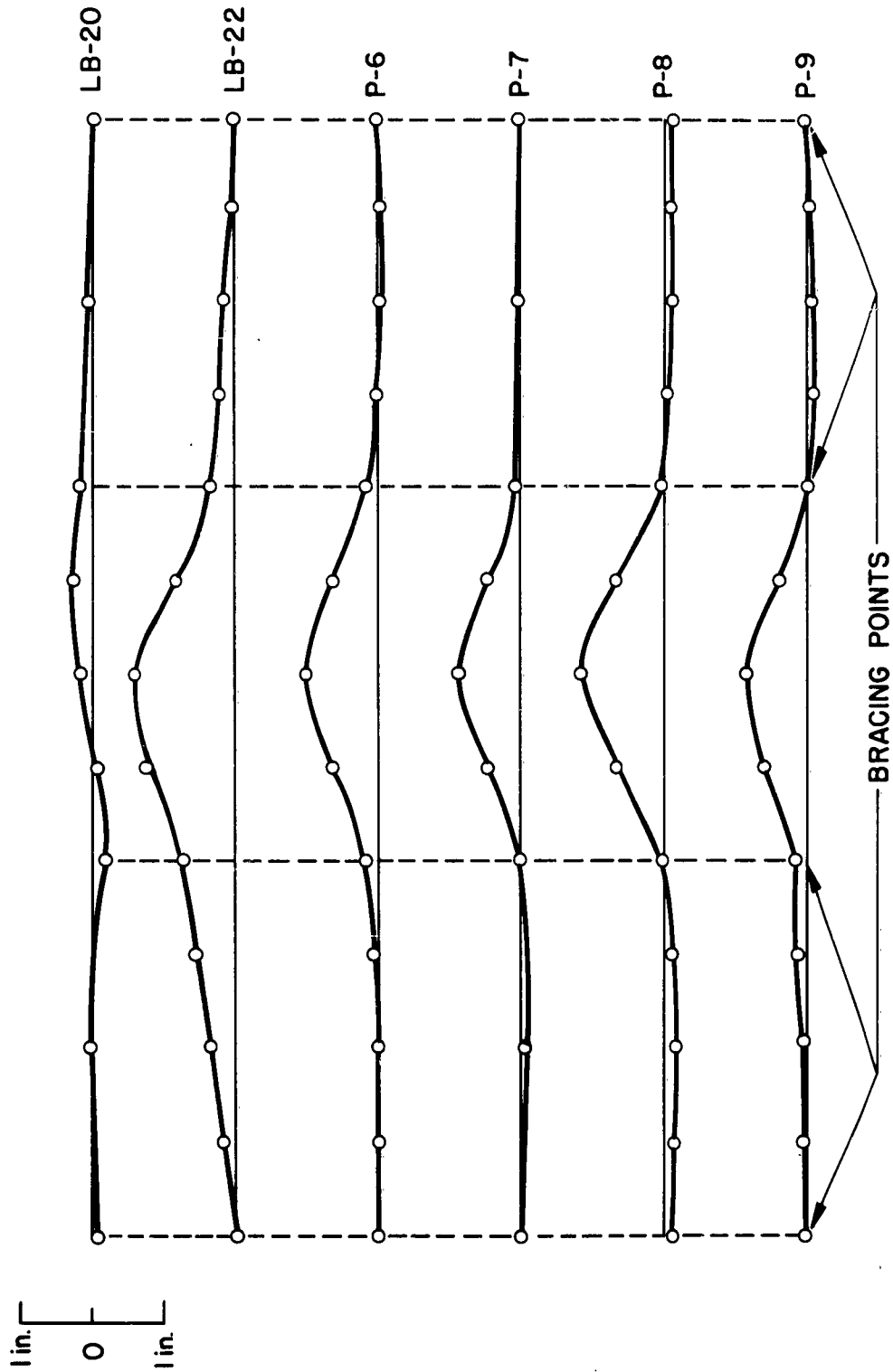


Fig. 21 Deflected Shapes of the Compression Flange,
Continued

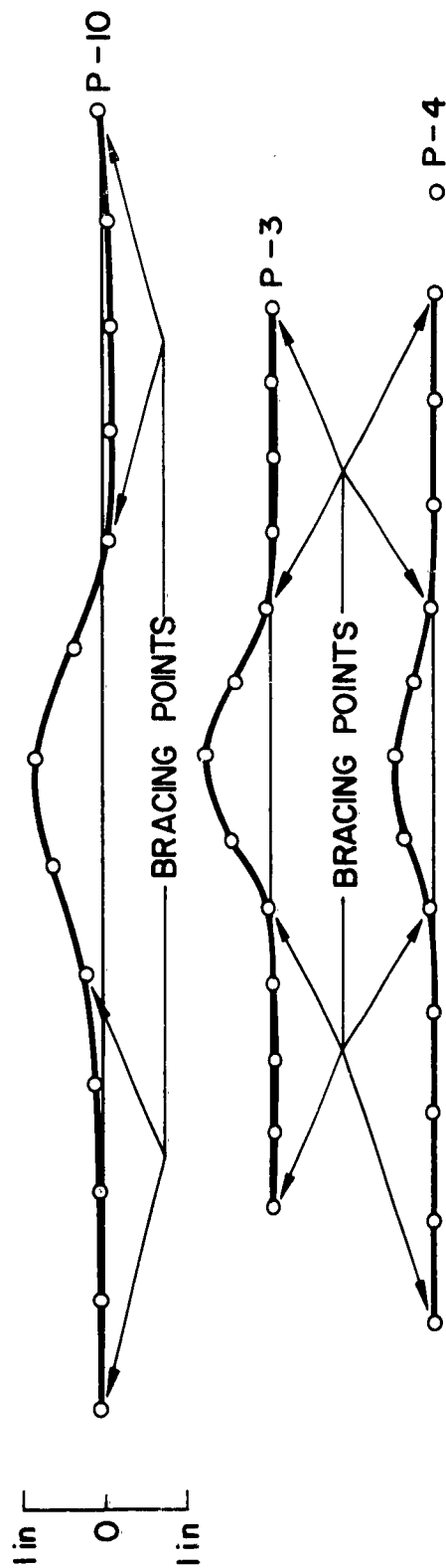


Fig. 22 Deflected Shapes of the Compression Flange,
Continued

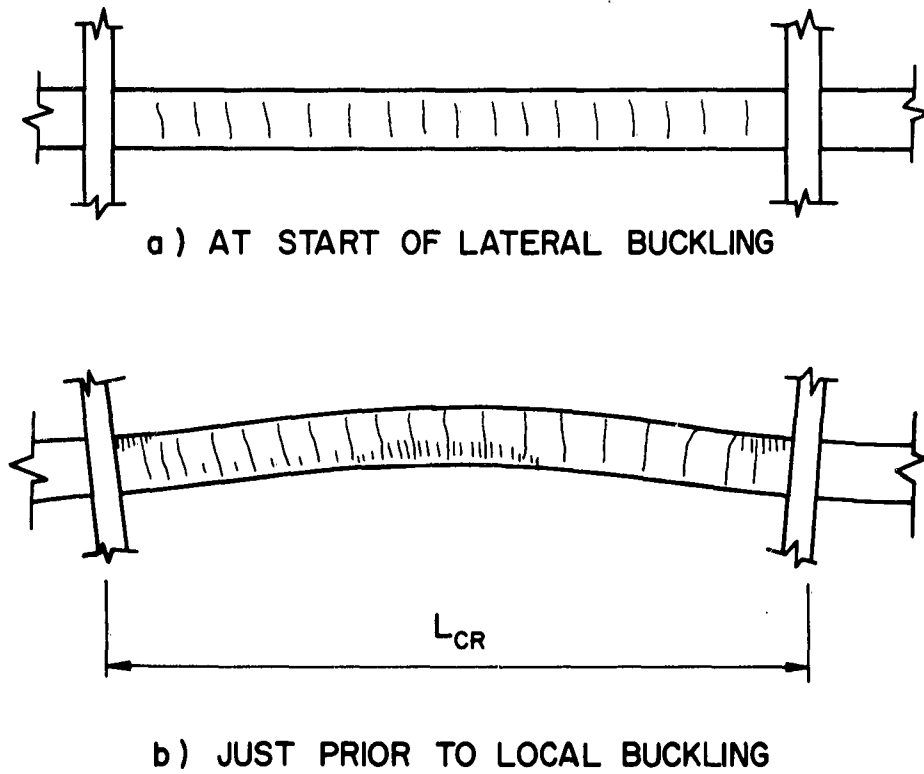


Fig. 23 Distribution of Yield Lines

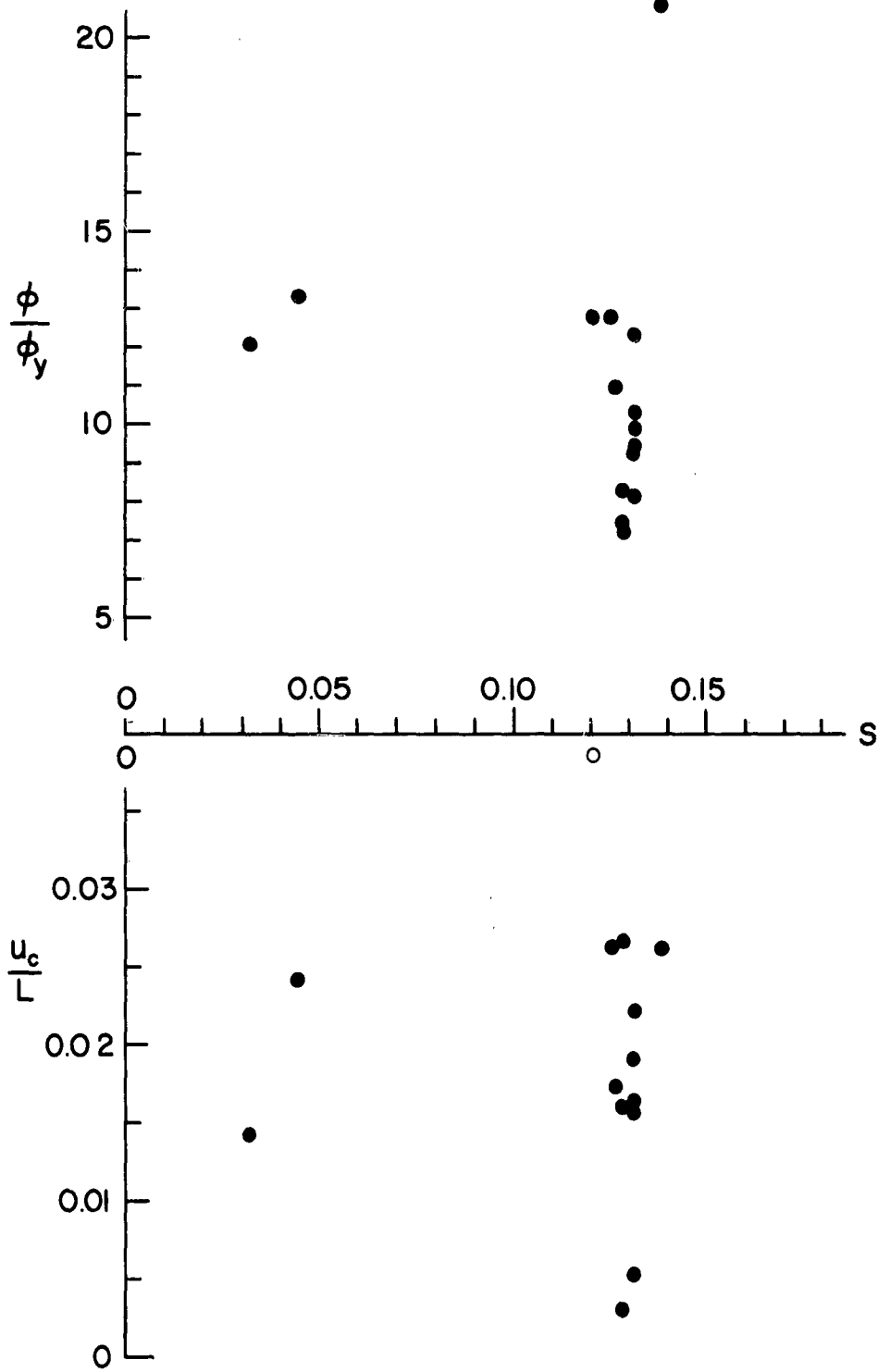


Fig. 25

Stiffness-versus-Deformations at Local Buckling

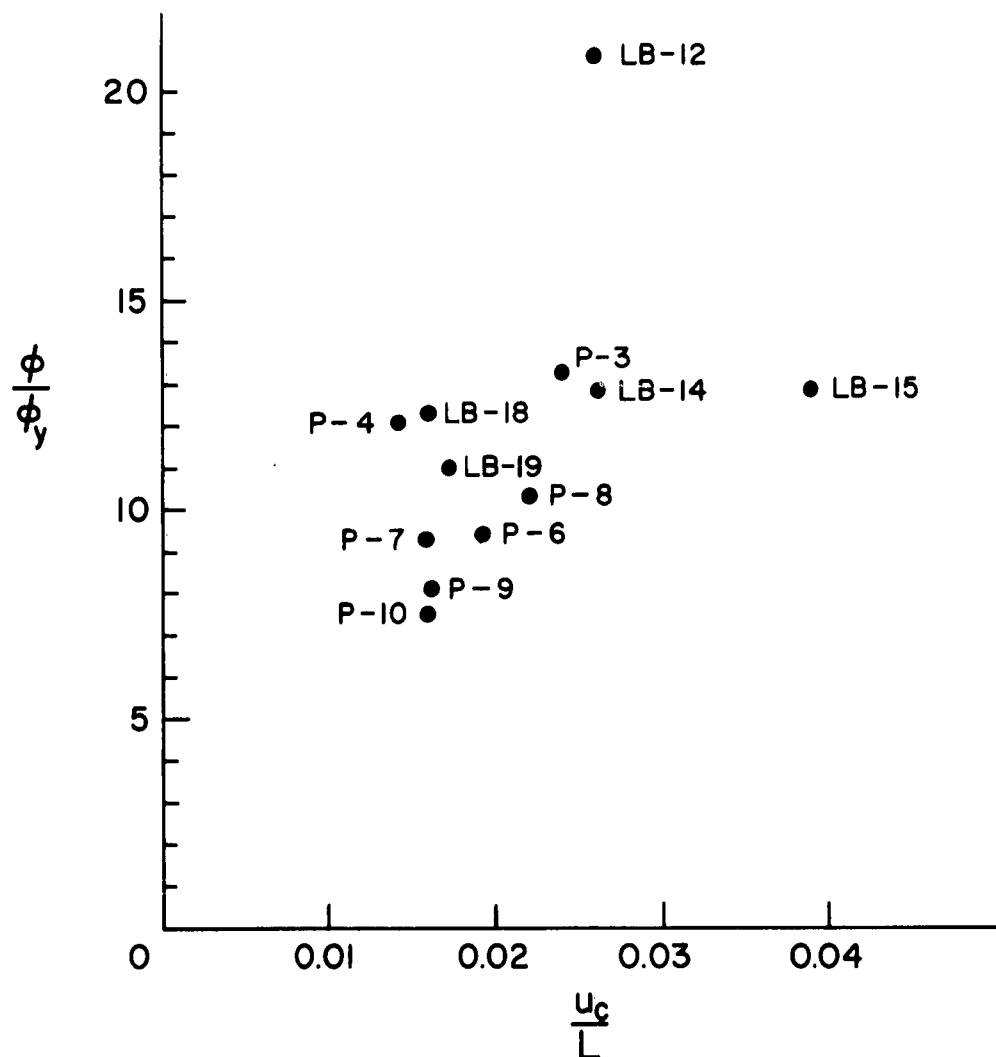
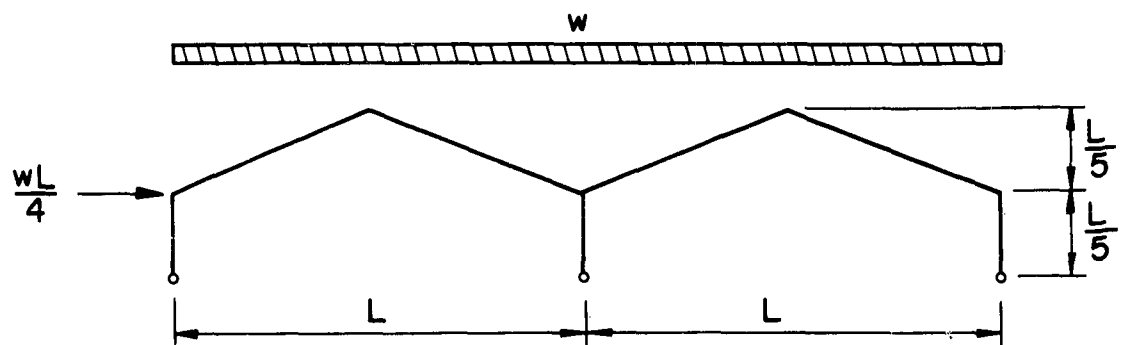


Fig. 26

Lateral-versus-Transverse Deformations
at Local Buckling



$L = 50' - 0''$;
ASTM-A7 Steel
All members are 16 WF 50

Fig. 27 Example Frame

8. REFERENCES

1. WRC-ASCE Joint Committee
COMMENTARY ON PLASTIC DESIGN IN STEEL
Chapter 5, "Verification of Plastic Theory"
ASCE Manual No. 41, 1961
2. G. C. Lee, T. V. Galambos
POST BUCKLING STRENGTH OF WIDE-FLANGE BEAMS
ASCE Proc. Paper 3059, Vol. 88, EM1, Feb. 1962
3. WRC-ASCE Joint Committee
COMMENTARY ON PLASTIC DESIGN IN STEEL
Chapter 6, "Additional Design Considerations"
ASCE Manual, No. 41, 1961
4. M. W. White
THE LATERAL-TORSIONAL BUCKLING OF YIELDED
STRUCTURAL STEEL MEMBERS
Ph.D. Dissertation, Lehigh University, 1956
5. G. C. Lee
INELASTIC LATERAL INSTABILITY OF BEAMS AND
THEIR BRACING REQUIREMENTS
Ph.D. Dissertation, Lehigh University, 1960
6. AISC
SPECIFICATION FOR THE DESIGN, FABRICATION
AND ERECTION OF STRUCTURAL STEEL FOR BUILDINGS,
PART 2
American Institute of Steel Construction,
Nov. 30, 1961
7. G. Winter
LATERAL BRACING OF COLUMNS AND BEAMS
ASCE Proc. Paper 2555, Vol. 86, ST 7, July 1960
8. W. Zuk
LATERAL BRACING FORCES ON BEAMS AND COLUMNS
ASCE Proc. Paper 1212, Vol. 83, EM2, April 1960
9. G. C. Driscoll, Jr.
ROTATION CAPACITY REQUIREMENTS FOR BEAMS AND
FRAMES OF STRUCTURAL STEEL
Ph.D. Dissertation, Lehigh University, 1958